Supplementary material

Contents

Section 1. Hazard layers and their definitions

1.1 River floods

The damages generated by flood inundation are estimated in various studies, mainly through hydraulic modelling and by quantifying socio-economic impacts of floods. The estimation is based on the concept of water depth-damage functions or loss functions and most of the literature considers direct tangible damage, which adds up most of total damage figure (Ward et al., 2011; te Linde et al., 2011). A central approach in economic damage is set on the monetary damage obtained from the type or use of the buildings or built-up space and the inundation depth. Several studies have focused on flood economic damage assessment across different scales, from river basins area (te Linde et al., 2011, Falter et al., 2016; Schumann et al., 2013) to pan- European (Lugeri et al., 2010; Feyen et al. 2012; Rojas et al., 2013; Alfieri et al., 2016) or even globally (Jongman et al. 2014). Similarly, loss of life is one of the most important consequences of flood disasters (Jonkman et al., 2016). River flooding studies are quantifying in most of the studies either the population affected as social damage (Rojas et al., 2013, Alfieri et al., 2016) or models the losses of life as a function of various variables (people at risk, mortality and evacuation fraction)(di Mauro et al., 2012; Kolen et al., 2012; Jonkman et al., 2016). The reported studies identify as the main driver of flood impact the increasing exposure (population, wealth, expansion of residential areas) in the flood prone areas (De Moel et al., 2011; IPCC, 2012, Elmer et al., 2012).

In order to provide an estimation of exposure (maximum potential impact) from floods, both on population and residential built-up, we use the European inundation maps derived by the high-resolution 2-D hydraulic model LISFLOOD (Bates et al., 2010; Alfieri et al., 2014) as a measure of the areal extent of the flood prone areas (fig. S1). The200 years return period hazard layer is considered. It is a low probability flood and it is proposed in the general floodplain legislation that defines the design flood (along with the 100 years return period) (Jakob, M., et. al., 2005). We intersect flood prone areas with built-up and residential population layers in order to determine the Flood management is based on prior assessments of flood events and their impacts. Such approach became dominant for flood control policies throughout Europe (Merz, B., et al., 2010). An approximation of the maximum potential impact, as suggested by our approach, can be a support to decision-making, in particular to prioritize areas where action is required.

Figure S1. River flood population (%) exposure (left) and the 200-year return period river flood hazard layer (right)

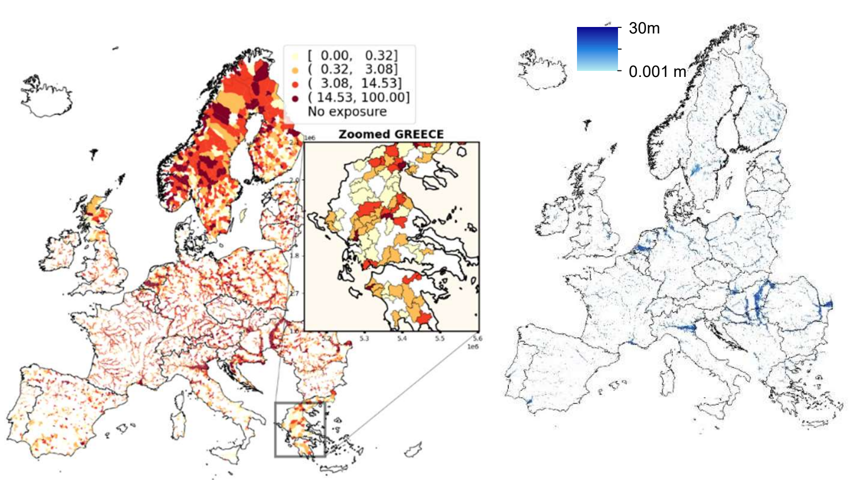

1.2 Landslides

Impacts from landslides on both built-up space (Zêzere et al. 2008, Papathoma-Köhle et al. 2011, Pomper et al., 2015) or human lives (Guzzetti, 2000, Papathoma-Köhle et al. 2007, Garcia et. al., 2016) are frequently considered respect to physical vulnerability (relationships between process intensity and the expected degree of loss) and social vulnerability assessments. In Europe, landslides are known for causing significant economic losses and less known for causing "catastrophic" events (loss of human life)(Papathoma-Köhle et al. 2007). Nevertheless, danger or threat from landslides occur when landslides as a natural process interacts with humans, their activities and/or properties (Jaedicke, C., 2014).

Landslides, as geohazard capable of causing damages, have been related in literature to either a hazard or a susceptibility map (Promper et al., 2016). For the RDH, we consider an 'hazard indicator' approach based on combining spatial and temporal probability layers. This is done by intersecting a landslide susceptibility layer from the ELSUS v2 (Wilde M., et al, 2017) with daily maximum precipitation from GPCC[1]. We follow here the methodology described in Thiebes et al., 2017. The resulting landslide hazard layer (fig. S2) combines the physical characteristics of various terrain factors that provides high predisposition to landslide occurrence with a probabilistic daily maximum precipitations using a matrix approach. For the purpose of our study, we have used the 200yr RP landslide hazard layer. In order to quantify the exposure from landslides we overlapped the hazard layer with assets layers (e.g. population ,residential built-up layers).

Figure S2. Landslide population (%) exposure (left) and the landslide hazard susceptibility layer (right)

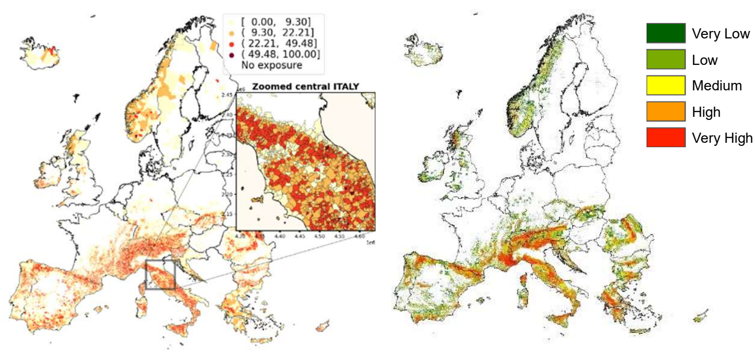

1.3 Coastal inundation

Coastal inundation (or coastal flooding) is generally defined as the sea water level that can exceed the height of natural (e.g., dunes, cliffs) or anthropic barriers (e.g., sea walls, dykes) (Vousdoukas, et al., 2016) producing catastrophic consequences in the coastal zones. Studies on coastal inundation have been related mainly with sea level rise (Lowe et al., 2009; Brown et al., 2012; Gaslikova et al., 2013) or as contribution of waves to sea water levels during extreme weather events (Barnard et al., 2015; Bertin et al., 2012; Vousdoukas, et al., 2016). The inundations impact on coastal zones has been considered either by quantifying flooded areas (Hinkel et al., 2014; Losada et al., 2013; Weisse et al., 2014) or by estimating the number of people affected as a direct or indirect proxy of coastal impacts (Brown et al., 2013; Hinkel et al., 2010; Lloyd et al., 2015). When combined with socioeconomic

[1] https://psl.noaa.gov/data/gridded/data.gpcc.html

exposure maps the coastal inundation estimation offers information with major implications for coastal management and adaptation.

For the present study, we used the estimated coastal flood extent with 200-year return period (fig. S3) developed by Vousdoukas, et al., 2016 in order to provide exposure of residential buildings and population to coastal flooding. The estimated inundation map represents the extreme total water level (TWL), and is the result of the contributions from the mean sea level (MSL), the tide and the combined effect of waves and storm surge. For a better description, please refer to Vousdoukas, et al., 2016 .

Figure S3. Coastal flood population (%) exposure (left) and the 200-year return period coastal flood hazard layer (right)

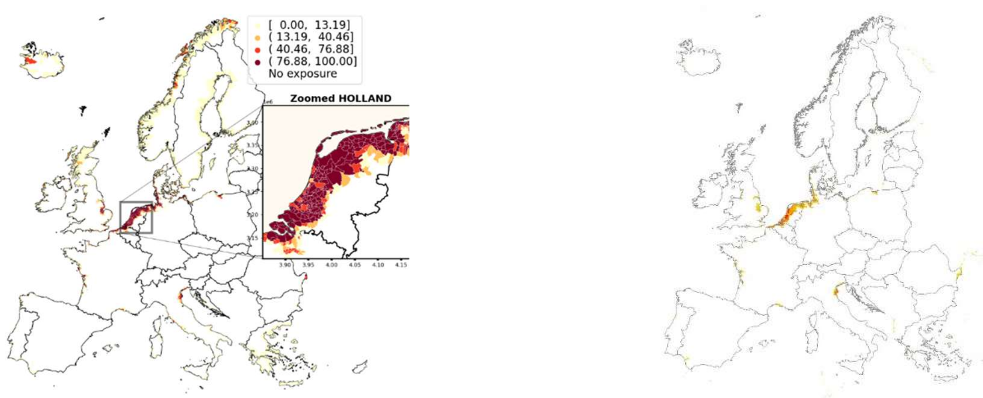

1.4 Earthquake

We identify the areal extend of the seismic hazard using the European probabilistic seismic hazard data produced in the context of the SHARE project (Woessner et al. 2015). More specifically we use the exceedance probabilities of peak ground acceleration (PGA) for a corresponding to 10 % exceedance probability in 50 years (i.e. equivalent to an average recurrence of such ground motions every 475 years).

In order to provide exposure from seismic hazard, we delineate in our study, areas from high intensity distribution with damage potential. We established these areas from an analogue approach that relates the physical ground motion parameters (such as PGA) with actual levels of damage derived from Instrumental Intensity scale developed by United States Geological Survey (USGS) (Worden, C. B., et. al., 2016). The intensity scale greater than 0.18 PGA or the equivalent “Moderate” potential damage level defines the areal confine we considered in our study. The intensity classes considered are shown in Table S1 (highlighted in grey):

Table S1. Instrumental Intensity scale developed by United States Geological Survey (USGS)

Instrumental Intensity	Acceleration (g)	Perceived shaking	Potential damage
I	< 0.0017	Not felt	None
II–III	0.0017 – 0.014	Weak	None
IV	0.014 – 0.039	Light	None
V	0.039 – 0.092	Moderate	Very light
VI	0.092 – 0.18	Strong	Light

VII	0.18 – 0.34	Very strong	Moderate
VIII	0.34 – 0.65	Severe	Moderate to heavy
IX	0.65 – 1.24	Violent	Heavy
X+	> 1.24	Extreme	Very heavy

Relating physical ground motion parameters with seismic intensities has been a difficult task for numerous studies either at worldwide level (Murphy, 1978; Trifunac and Brady 1976), European wide level (Corbane, et.a al., 2017), regional (Wald, D. J., et. al., 1999,) and country level (Teselentis, G., A, et. al., 2008, Faenza, L., et al., 2010). It is an ideal alternative solution as the intensity of an earthquake is not entirely determined by its magnitude but is rather empirically based on observed effects of the earthquakes (Musson, R., M.,W.,2000). Nevertheless, an equation that expresses the relationships between seismic intensity and PGA applicable uniformly across EU countries is difficult to identify (Corbane, et.a al., 2017). Therefore, by using the USGS's Instrumental Intensity scale greater than 0.18 PGA, equivalent to "Moderate" potential damage level we have approximated areas with potential impact from seismic hazard at European level. Within these areas, we have quantified the residential build-up and population exposure to the seismic hazard (fig. S4). We did not disaggregate, within the considered seismic hazardous area, the attributes of residential build-up and population in order to search for elements most likely to be damaged/impacted. Instead, we have assessed the residential build-up and population sums and densities within the seismic hazardous area. Consequently, the exposure and its variability is expressed as sum (absolute value) and as densities (relative values) of residential build-up and population among the cumulative statistical areas (LAU) situated in the areas prone to seismic hazard .

Figure S4. Population (%) exposed to earthquake aggregated at LAU level (left) and the earthquake hazard layer (right)

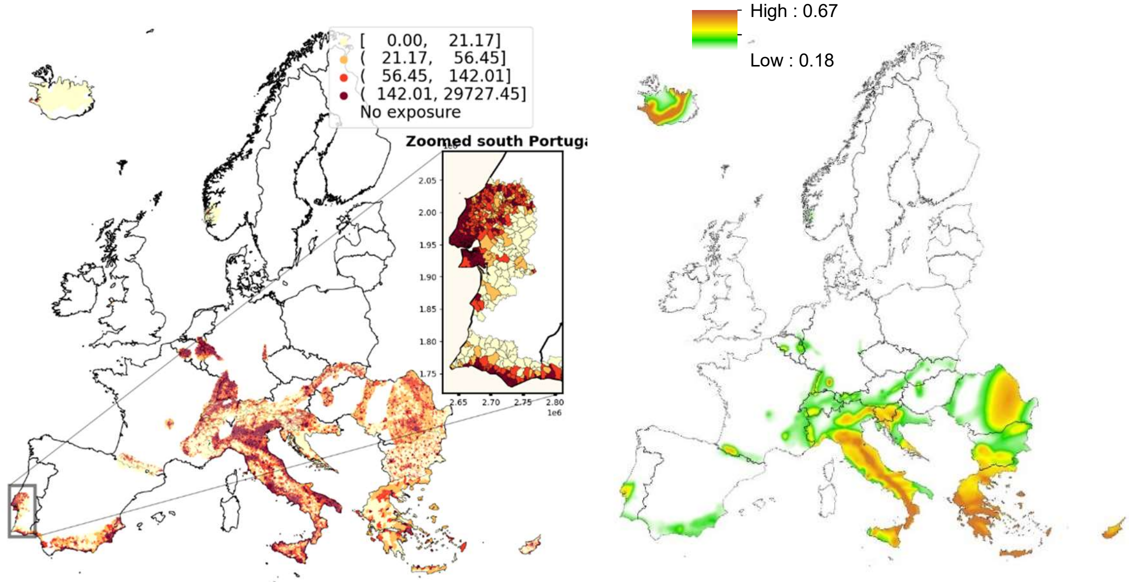

1.5 Drought (Subsidence)

Here we define subsidence as a clay-related geohazard capable of causing harm to both life and the built environment. It is a result of soils shrinking and swelling according to wetting and drying conditions respectively (Corti et al. 2011) which causes vertical and horizontal ground movement (due to volumetric changes in soil mass) causing significant damage to buildings and infrastructure (Pritchard, et. al., 2015). Ground movement, incorporating clay-related subsidence, is a recognised hazard across some EU member countries: UK (Cabinet Office 2011), France (JORF, 1992) or in USA (Seed, et.al., 1962, Van der Merve, D.H., 1964). It is a highly damaging geohazard: Corti et al., (2011) suggests that the impact of soil subsidence in France is exceeding, financially, flooding, Sudjianto et al. (2011), Steiberg, (2008) in the United States, suggests that the financial cost of swelling soils has exceeded other natural disasters (i.e. tornadoes, earthquakes and hurricanes) and Pritchard, et. al., 2015 suggests that clay-related subsidence is Great Britain's (GB) most damaging soil-related geohazard, costing the economy up to £500 million per year.

In our study, we aimed to provide a measurable and geographically defined potential impact areas from clay-related subsidence. Our approach does not quantify the shrink–swell behaviour of a soil by modelling meteorological, soil hydrology or soil mechanics data. Instead, we indicate the potential for such a hazard to be present, with regard to the amount of clay content of the soils on which the high activity and plasticity index of the soils is based on. Likewise, in order to nominate soils that are prone to subsidence (shrink-swell) at European level we have extracted from the Dominant surface textural class of the STU (ESDAC), the soils with values of fine and very fine soil texture and with clay content greater than 35%. Atkinson, J., 2014, suggests that the proportion of clay mineral flakes (< 2 mm size) in a fine soil affects its current state, particularly its tendency to swell and shrink with changes in water content. This happens because - in the case of fine soils (such as soils with high content of clays) - it is the shape of the particles rather than their size that has the greater influence on engineering properties of the soil. Clay soils are characterised by flaky particles to which water adheres, thus imparting the property of soil plasticity. Consequently, we have defined the soils with fine texture and clay content greater than 35% as soils with high subsidence potential and based on their geographical extent and location we have mapped the subsidence susceptibility area at European level (fig. S5).

Figure S5. Population (%) exposed to subsidence aggregated at LAU level (left) and the subsidence hazard layer (right)

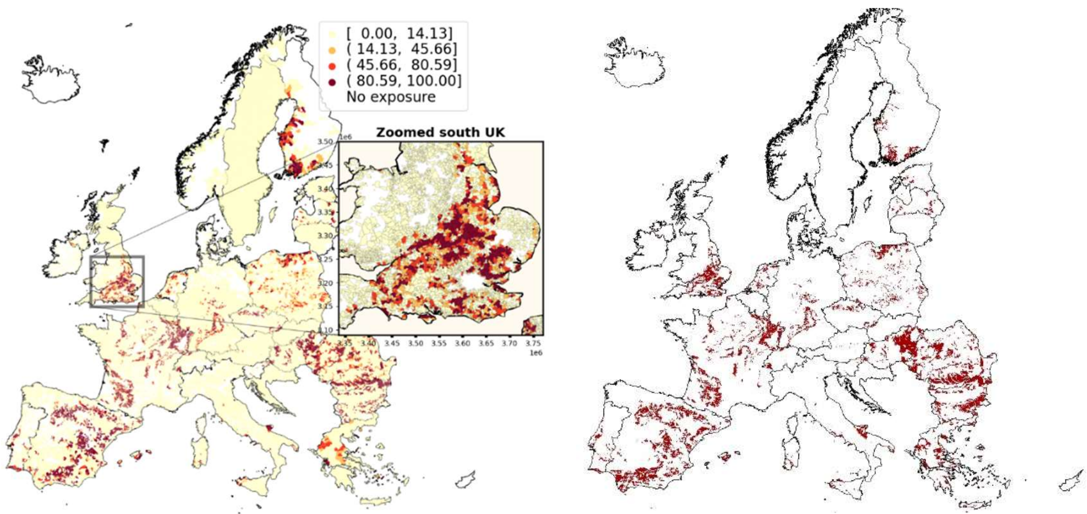

1.6 Forest Fire

Forest Fire has been described using a variety of approaches and variables including expected fire behavior (Hardwick et al., 1998; Hessburg et al., 2007), fuel characteristics (Hogenbirk and Sarrazin-Delay, 1995), satellite image classification (Cohen, 1989; Jain et al., 1996; Ercanoglu et al., 2006), topography analysis (Yool et al., 1985), expert knowledge (Gonzalez et al., 2007), crown fire index calculations (Fiedler et al., 2003) and identification of Wildland-Urban Interface (Bar-Massada et al., 2014; Cohen, 2000; Lampin-Maillet et al., 2009; Lowell et al., 2009).

For the current study, in order to find the hazardous potential of forest (wild) fire, we considered Wildland–Urban Interface area (WUI) (FAO, 2002), as areas where wildfires are most likely to threaten assets and population and present fire danger conditions.

Identification of WUI areas that are more likely to be affected by fires is essential for fire management. Researchers and policymakers have requested for a better accountability of impact potential from fire hazard especially within the WUI areas communities (Lee, 1991; Jakes, Kruger, Monroe, Nelson, & Strurtevant, 2007).

Accordingly, population (Johnson Gaither, et. al. 2015; et. al., 2011; WFEC, 2014) or artificial areas (Atkinson, et al., 2012; Chuvieco et al., 2010; Keane, et. al., 2010; Stockmann, et. al., 2010) has been largely used for characterising potential exposure or sensitivity to forest fire within the WUI areas. Conducted at relevant spatial scales, fire hazard potential in the WUI area can provide important information about the magnitude and extent of impact.

A threefold steps approach was set in our study for characterising potential exposure and sensitivity to forest fire. First, we identified the WUI areas at European level, then we delimited the WUI area with potential fire activity and lastly we quantified the residential built-up area and population exposed to fire within the identified WUI area.

In the first step the WUI areas at European level are mapped according to the methodology described by [Modugno., S. et. al, 2016]: as the space where artificial surface (build-up area) and forest fuel mass come into contact. These two surfaces were created as the selection from level 1 and 3 land cover classes from CLC 2006 shown in Table S2.

Table S2. CLC 2006 nomenclature used to select classes that represent the residential areas and fuel areas

Residential areas	Code	Fuel areas	Code
Continuous urban fabric	1.11	Broad-leaved forest	3.11
		Coniferous forest	3.12
Discontinuous urban fabric	1.12	Mixed forest	3.13
		Sclerophyllous vegetation	3.23
		Transitional woodland-shrub	3.24

The maximum buffer distances - according to the Mediterranean Countries forest fire management plans (add ref here) - around the considered fuel and artificial surfaces were used, ensuring in this way that no area exposed to forest fire is overlooked. The considered buffer distances around the artificial and fuel areas were, likewise, set as 400 m from fuel mass (woodland) and 200 m from urban space. Finally, to account for WUI areas, the intersecting artificial surfaces and the fuel surface buffer zones are mapped. Fig. S6 depicts the geospatial analysis method used.

Figure S6. GIS analysis to generate WUI areas (Modugno, S., et. al, 2016)

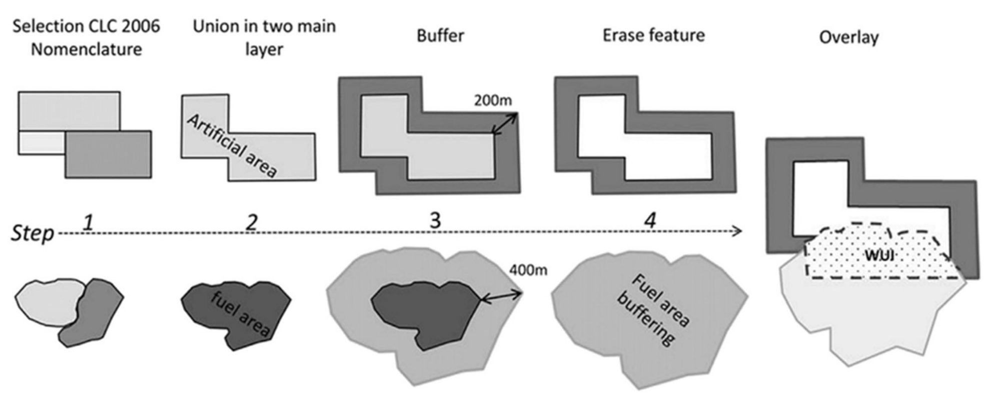

In order to identify the WUI area with potential fire activity, we established a spatial relationship with historical events (burned areas) as a function of the distance from the historical burned area. The historical event database of burned areas used cover the period 2006-2017 and was accessed from the Joint Research Centre European (San-Miguel-Ayanz et al., 2013) product, supplied by the Forest Fires Information system (EFFIS, 2014). A Euclidean distance of 10 km was applied and considered as independent explanatory variable for the potential fire activity. More detailed methods using logistic regression (LoR), modelled the relationship between burned area and WUI areas (Martinez et al., 2009, Vilar et al., 2010, Kleinbaum and Klein, 2010, Modugno., S. et. al, 2016) and established the 10 km limit range from the burned areas as hypothetical distance with increased probability of fire activity. By applying this distance range, we have selected the WUI areas with high potential fire activity at European level (fig S7).

Lastly, we quantify the exposure of residence-build up and the residential population when their location intersects the WUI areas with high potential impact (fig S7 - right).

Figure S7. Population (%) exposed to subsidence aggregated at LAU level (left) and the subsidence hazard layer- WUI areas with high potential impact (right)

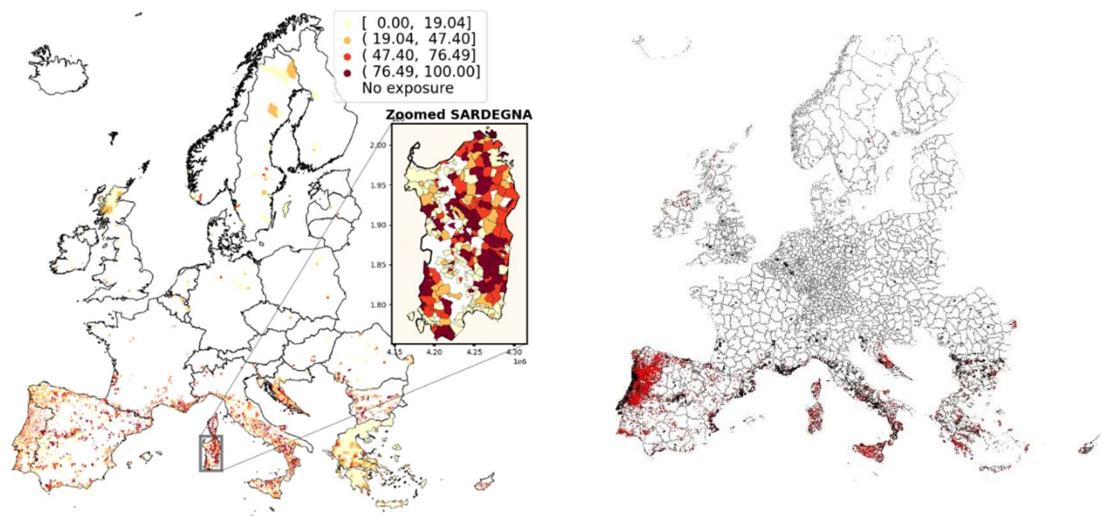

Section 2

2.1 Maximizes the autocorrelation/clustering

Based on the selection of the neighbourhood size (*k*) in the k-Nearest Neighbour the spatial autocorrelation/clustering across single hazard exposures can be maximized. In the k-NN literatures, there are several studies focusing on the selection of an optimal *k* for k-Nearest Neighbour (Hand, D.J. et all 2003; Gosh, A. K. et all 2006; Hall, P. et all 2008). The optimal *k* value has to balance between susceptibility to noise and outliers for low values (large z-scores with high variance) and risks of over-smoothing for high values (small z-scores with low variance).

A variety of techniques are available to determine the optimal *k* value for clustering algorithms (Tibshirani et al., 2001, Rousseeuw, 1987, Baker and Hubert, 1975, Smyth, 1996) and various ways of being categorised, either if we consider their application on clustering geographical neighbours (in conceptualisation of spatial relationship as it is in our case) or on clustering attributes of neighbours (referring to text mining or machine learning). Generally, they are grouped into three classes of criteria (Theodoridis and Koutroubas, 2008): (i) relative (compare two different clustering or clusters), (ii) external (evaluation of a clustering structure by comparing it with other clustering schemes) and (iii) internal criteria (evaluation based on the internal clustering structure).

Our approach falls into the internal criteria technique and is based on the effect of the size of *k* by running a clustering algorithm (a spatial lag model with k-Nearest Neighbour spatial weight matrices in our case) several times increasing the stepwise *k* value for each run. This method is central to the geostatistical concept of variogram, which gives the variation of sites' attribute as distance between sites increases. We run the clustering algorithm 10 times increasing the stepwise k=5 for each run. The coefficients we used to investigate the variations among clusters are: Mean Square Error (MSE), Correlation coefficient and within cluster sum of squared errors (WCSS) (fig S8). We also used and an empirical rule-of-thumb popularized by the "Pattern Classification" book by Duda et al., 2001 which sets the *k* equal to the square root of the number of instances.

The procedure of identifying the optimal *k* parameter is based on "elbow" method (Aldenderfer, et all 1984). The method used is a visual method and involves graphing the coefficient on a y-axis and the number of increasing stepwise clusters on an x-axis. It shows that increasing the number of clusters improves the fit (the variation is better explained) and it is represented either through increasing correlation or through decreasing error. A marked flattening of the graph suggests that the clusters being created are over-fitted, thus the appropriate number of clusters is found at the 'elbow' of the graph (Ketchen, et all. 1996).

The optimal number of neighbours (*k*) around the individual regions (LAU) that optimize the clustering are presented in Table S3 and Table S4. The method is applied on population and residential build-up, both on absolute and relative aggregations of the exposure to the considered hazards.

Figure S8. Elbow method applied on 3 coefficients used to investigate the optimal k: MSE (upper left), Correlation coefficient (bottom left), WCSS (upper right). The plots indicate the optimal number of neighbours (*k*) to be used to maximize the relative population exposed to landslides clustering (as identified by the 3 coefficients) *(Please see fig. 11 to 21 for the built-up and population plots)*

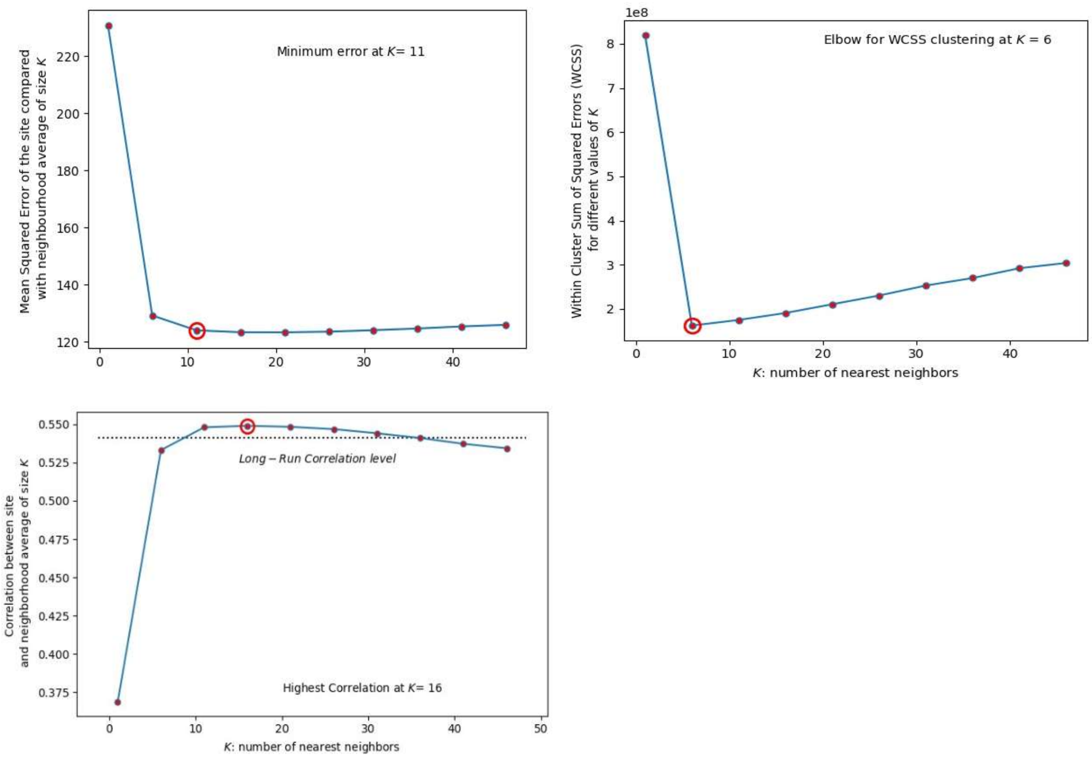

Table S3. The optimal neighbourhood size (*k*) of the population (absolute and relative) exposures identified by the coefficients Mean Square Error (MSE), Correlation , Within Cluster of Sum of Squared errors (WCSS) using the "elbow" method

Coefficient	WCSS		Correlation		MSE	
Hazard / Aggregation	Absolute	%	Absolute	%	Absolute	%
Coastal flood	6	11	16	6	16	6
Earthquake	6	6	16	1	16	1
River flood	6	11	21	6	21	11
Landslide	6	6	16	16	16	11
Subsidence	6	6	6	6	11	6
Forest fire (WUI)	6	11	21	6	41	11

Table S4. The optimal neighbourhood size (*k*) of the residential build-up (absolute and relative) exposures identified by the coefficients Mean Square Error (MSE), Correlation , Within Cluster of Sum of Squared errors (WCSS) using the "elbow" method

Coefficient	WCSS	Correlation	MSE

Hazard / Aggregation	Absolute	%	Absolute	%	Absolute	%
Coastal flood	6	6	16	6	16	11
Earthquake	6	6	6	6	11	6
River flood	6	6	21	6	21	11
Landslide	6	6	16	11	16	11
Subsidence	6	36	11	6	11	6
Forest fire (WUI)	6	11	11	6	11	11

We compare the distributions of the effect size (z-score) and their significance level for the single hazard exposures in order to choose the optimal number of neighbours *k* detected previously by the coefficients Mean Square Error (MSE), Correlation and Within Cluster of Sum of Squared errors (WCSS). We observe (as the example presented in fig. S9) a general agreement on 3 among the 4 methods (the 'thumb' method appears dissimilar) which indicate that any *k* identified by these methods would optimize the clustering similarly. We select the number of *k* neighbours identified by the correlation coefficient, to optimize the clustering and perform the hotspots analysis for the single hazard exposures.

Figure S9. The distribution of the effect size (z-score) (upper plot) and the significance (bottom plot) of the methodologies used to compute the optimal *k* for the single hazards considered (example of the relative (%) population exposure). Please see below in fig. 22 the same for the built-up exposure (%)

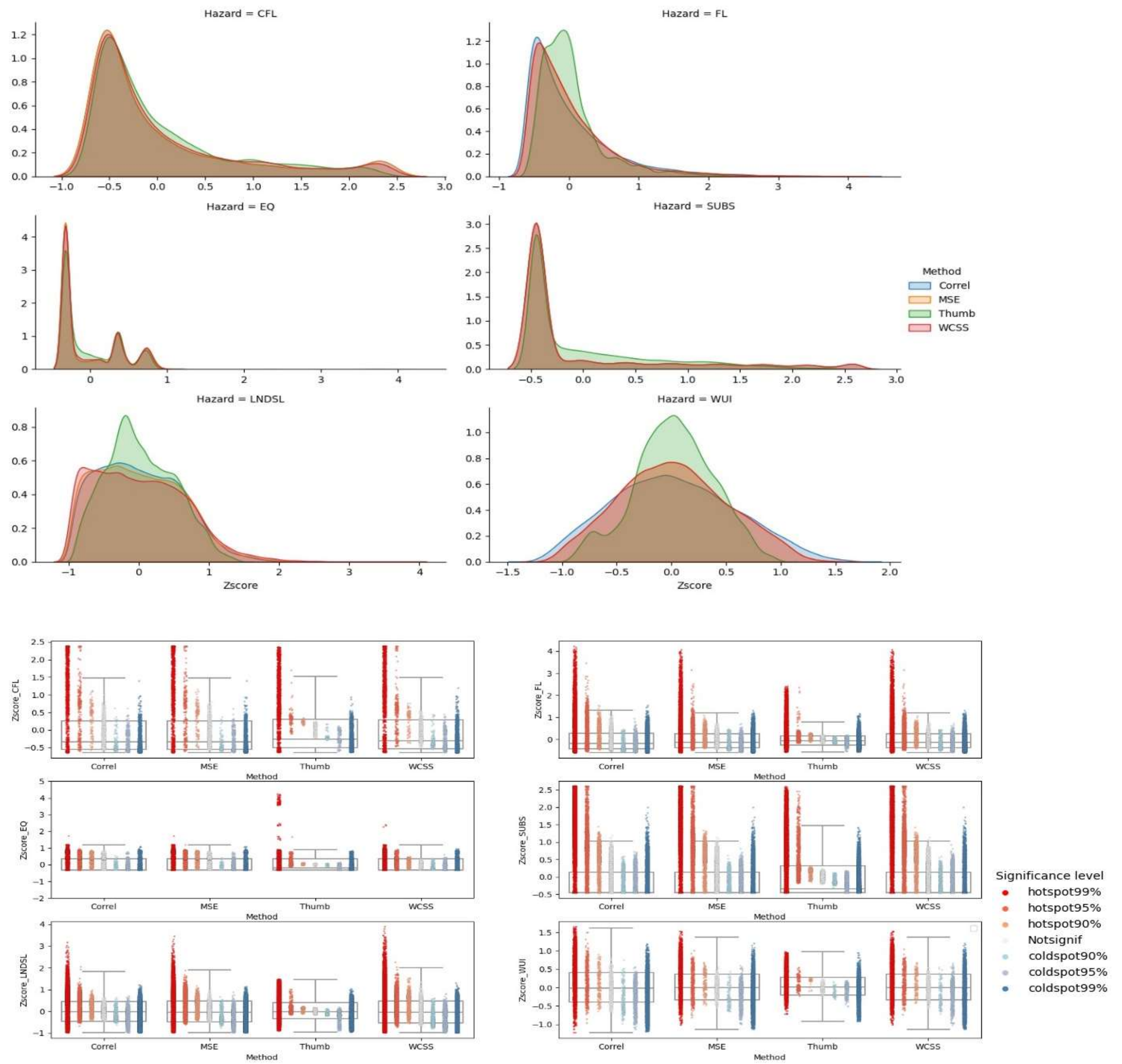

Once the hotspot analysis is completed for the single hazards both for residential area and population grids, the resulting clusters with various significance levels are combined in a multi-hazards hotspot analysis.

Figure S10 . Elbow method applied on ***Correlation coefficient.*** The plots indicate the optimal number of neighbors (*k*) to be used to maximize clustering of the relative (%) population exposed to : coastal flood, flood, subsidence clustering (left side from upper to bottom plots) earthquake, landslides, forest fire_ WUI clustering (right side from upper to bottom plots)

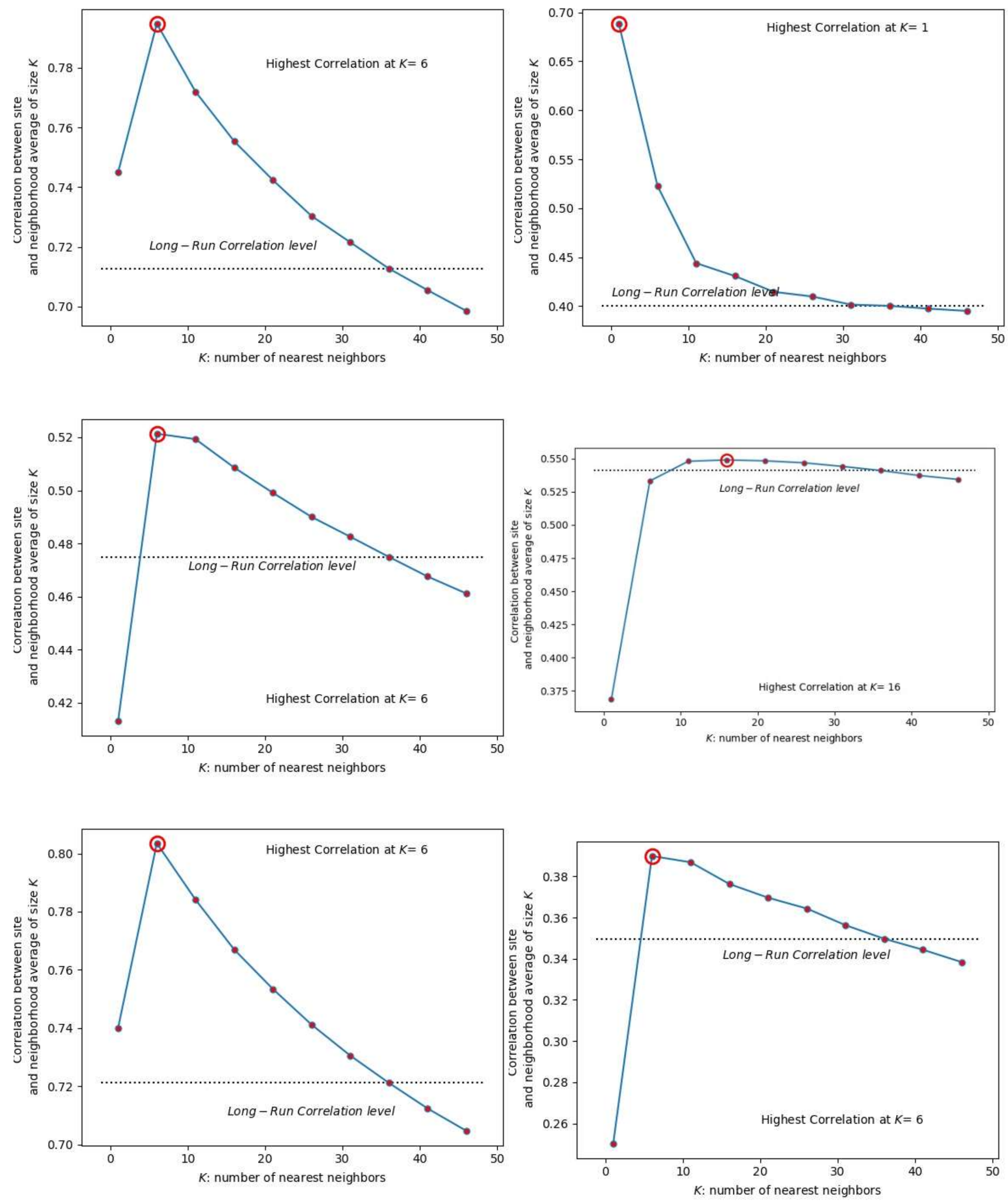

Figure S11 . Elbow method applied on Correlation coefficient . The plots indicate the optimal number of neighbors (*k*) to be used to maximize the clustering of (absolute) population exposed to : coastal flood, flood, subsidence clustering (left side from upper to bottom plots) earthquake, landslides, forest fire_ WUI clustering (right side from upper to bottom plots)

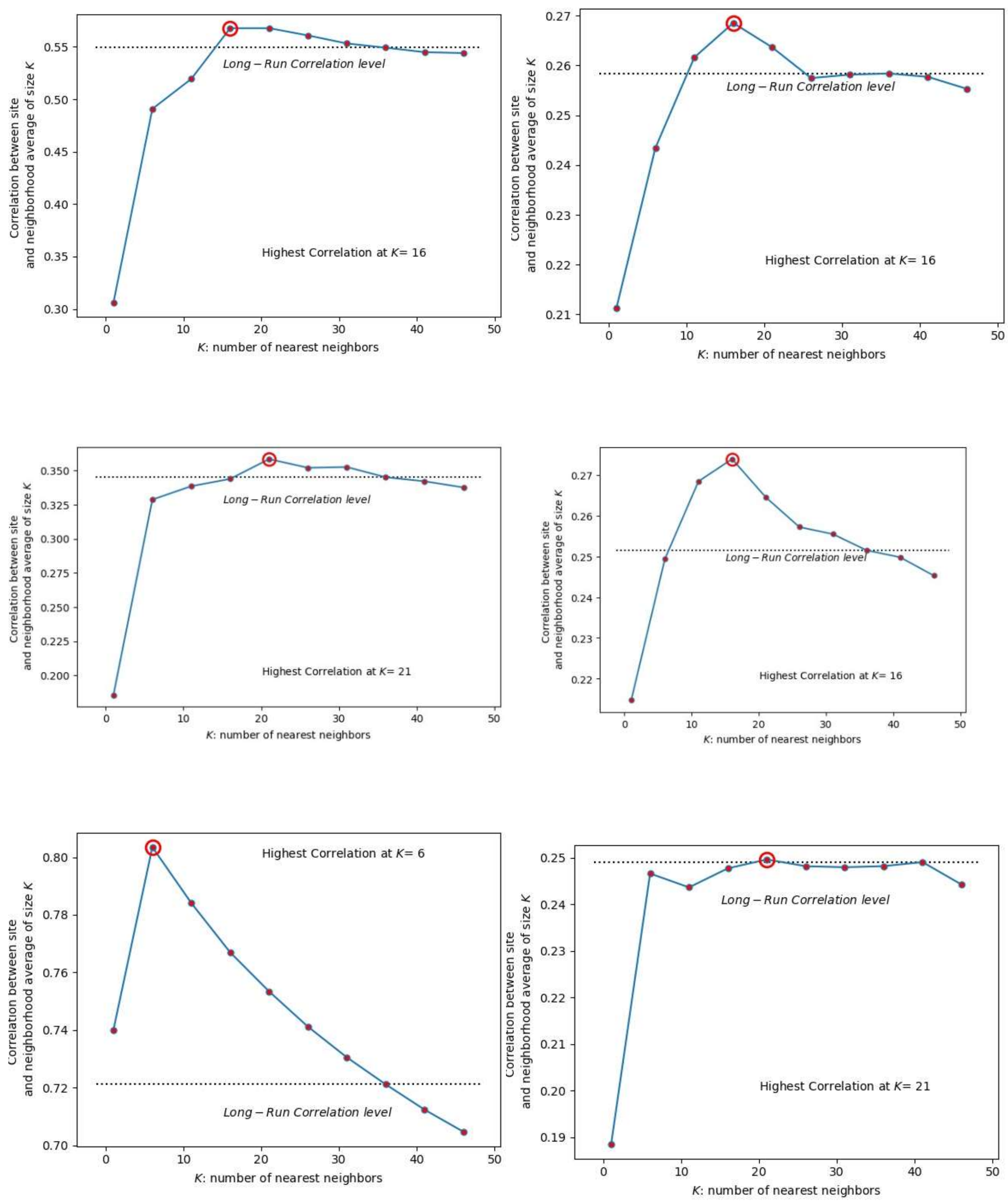

Figure S12 . Elbow method applied on Correlation coefficient. The plots indicate the optimal number of neighbors (k) to be used to maximize clustering of the relative (%) residential buitlup exposed to : coastal flood, flood, subsidence clustering (left side from upper to bottom plots) earthquake, landslides, forest fire_ WUI clustering (right side from upper to bottom plots)

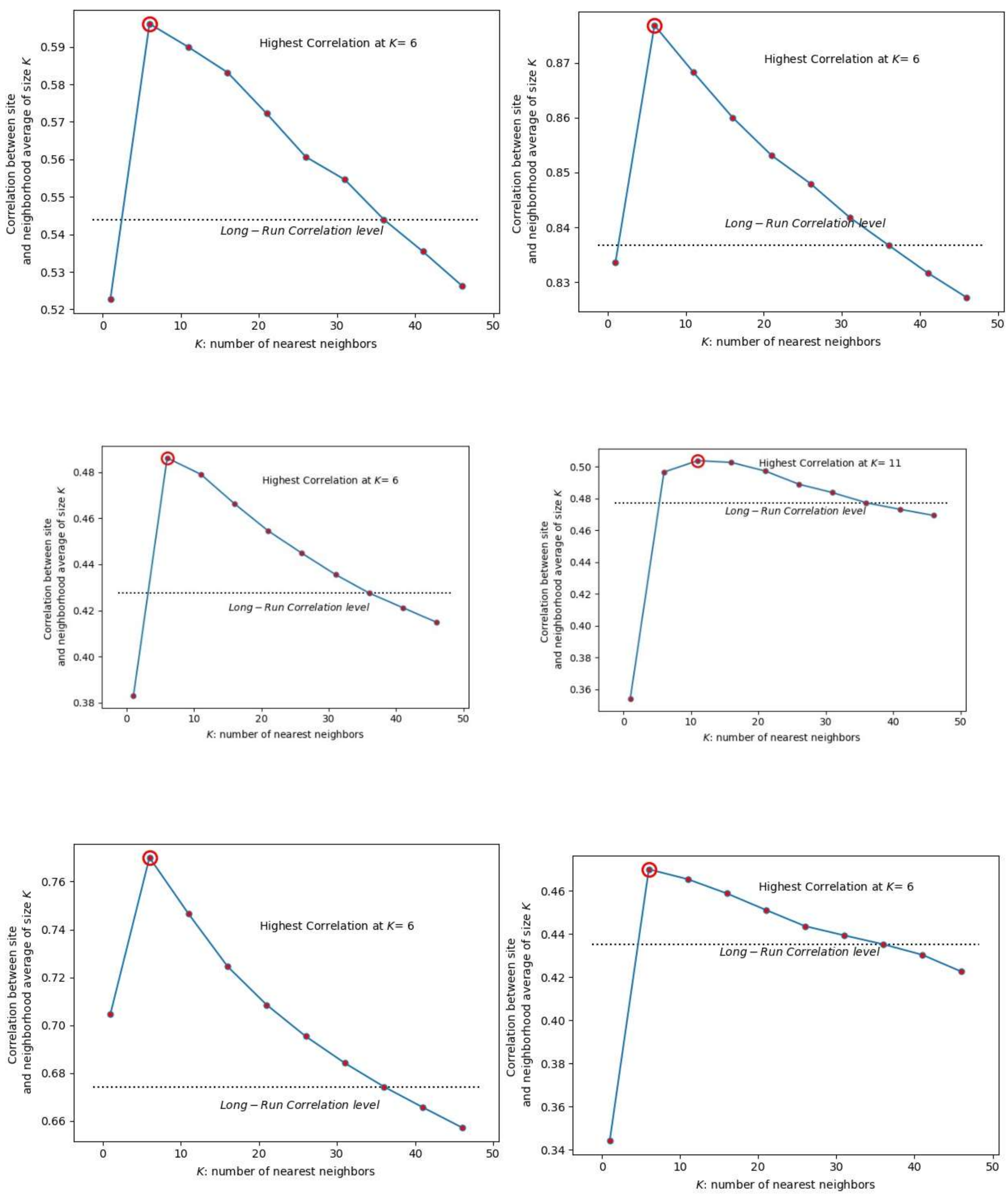

Figure S13 . Elbow method applied on Correlation coefficient. The plots indicate the optimal number of neighbors (k) to be used to maximize clustering of the absolute residential built up exposed to : coastal flood, flood, subsidence clustering (left side from upper to bottom plots) earthquake, landslides, forest fire_ WUI clustering (right side from upper to bottom plots)

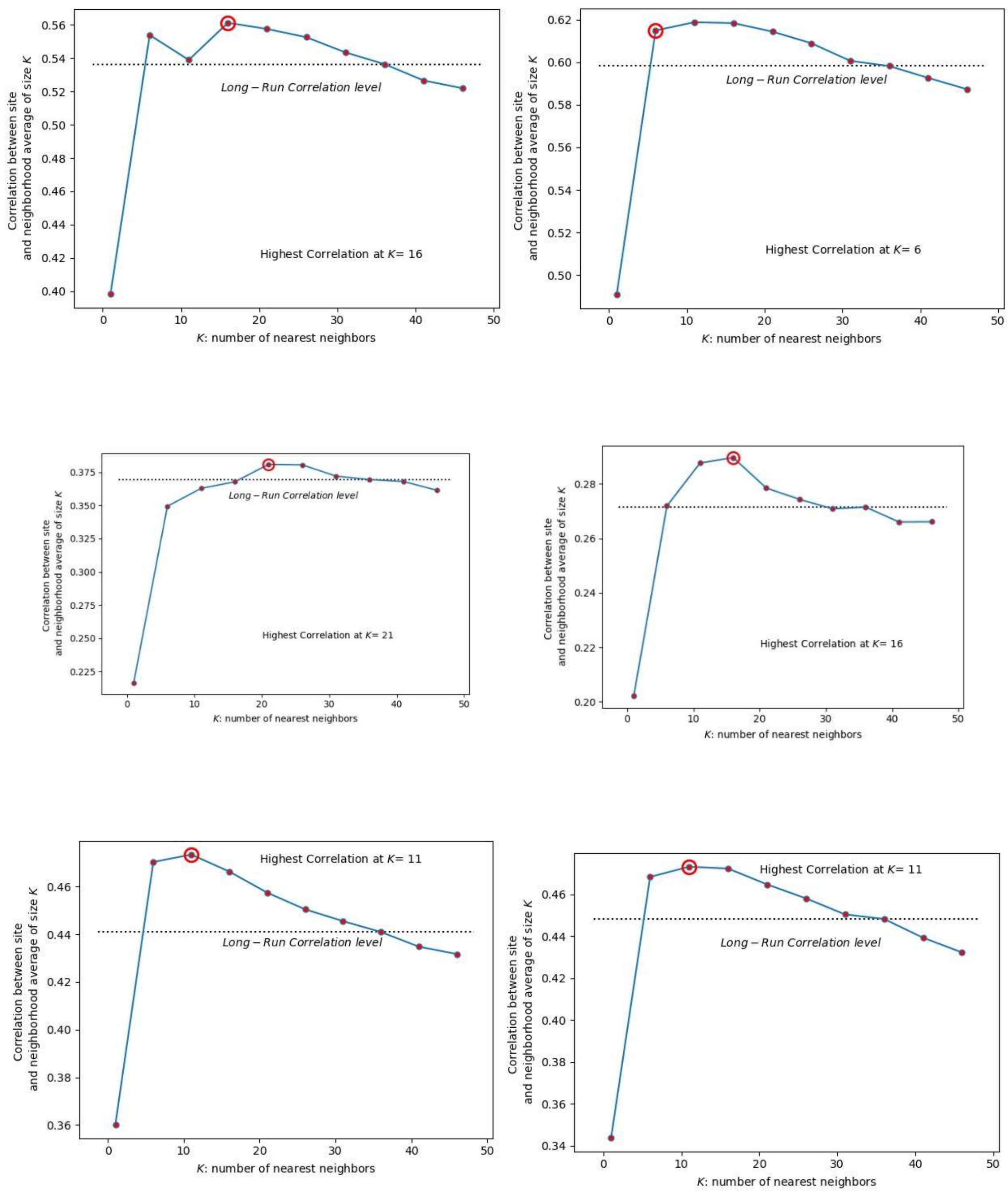

Figure S14 . Elbow method applied on **WCSS coefficient**. The plots indicate the optimal number of neighbors (k) to be used to maximize clustering of the relative (%) population exposed to : coastal flood, flood, subsidence clustering (left side from upper to bottom plots) earthquake, landslides, forest fire_ WUI clustering (right side from upper to bottom plots)

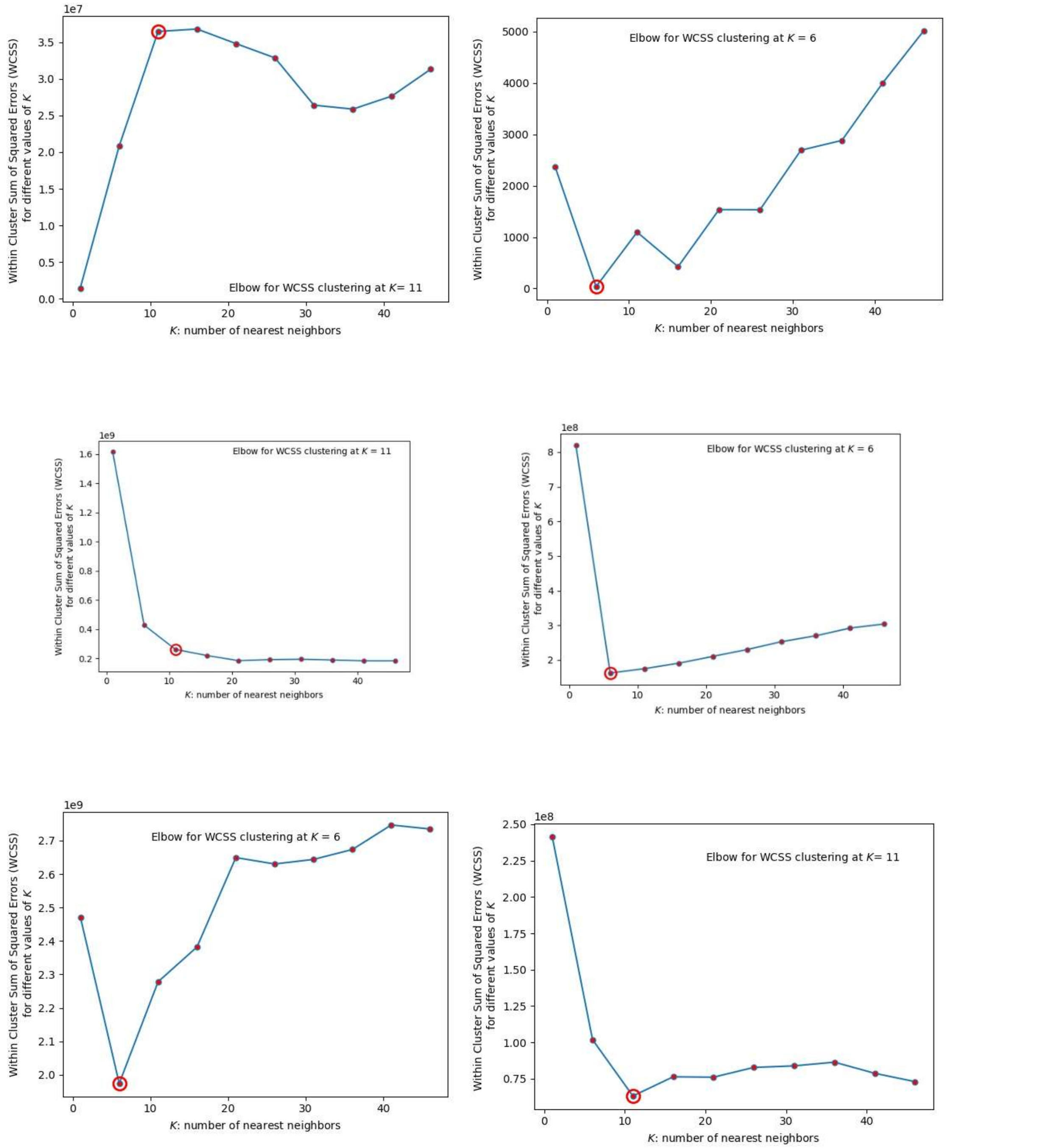

Figure S15 . Elbow method applied on **WCSS coefficient**. The plots indicate the optimal number of neighbors (k) to be used to maximize clustering of the absolute population exposed to : coastal flood, flood, subsidence clustering (left side from upper to bottom plots) earthquake, landslides, forest fire_ WUI clustering (right side from upper to bottom plots)

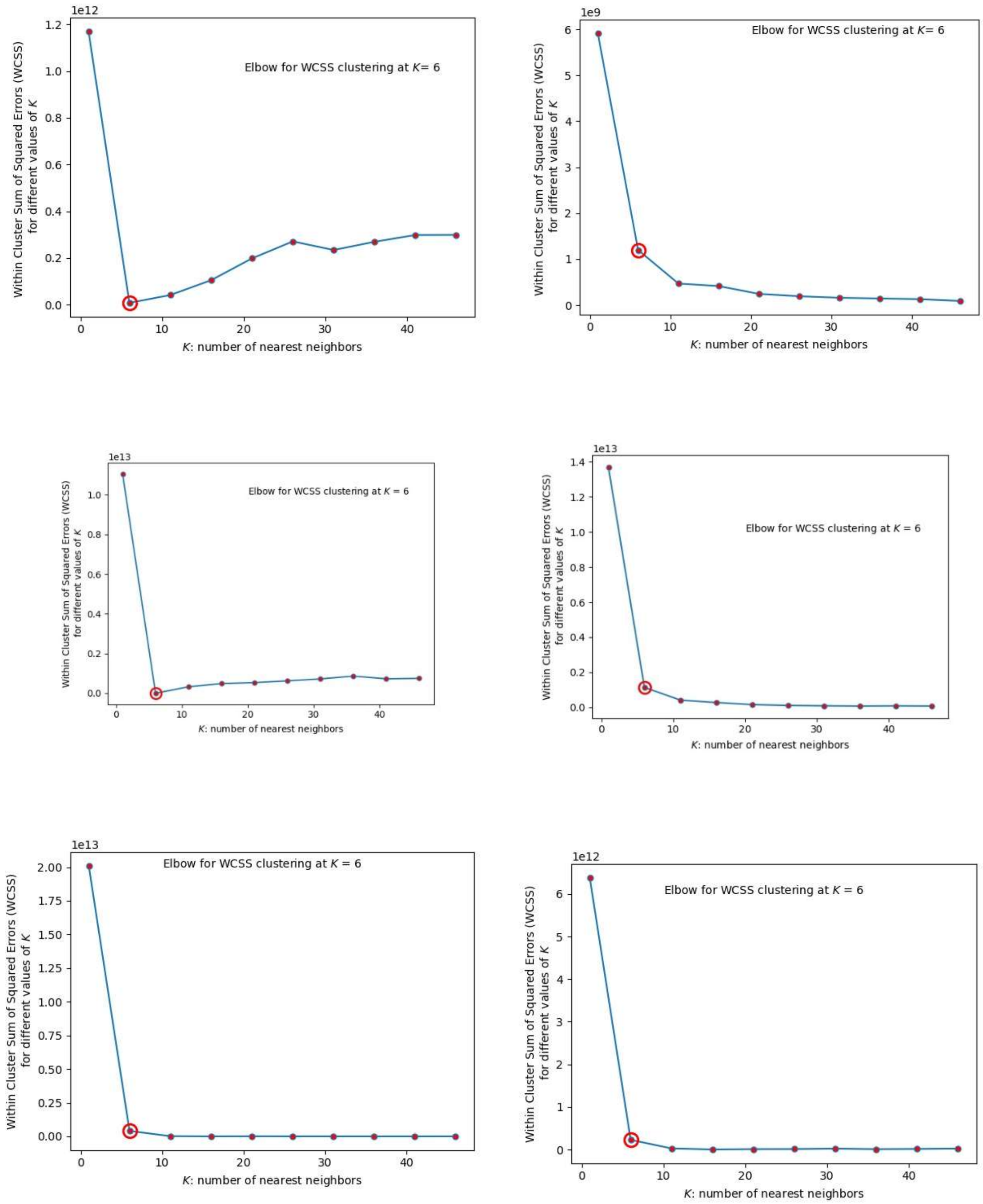

Figure S16. Elbow method applied on **WCSS coefficient**. The plots indicate the optimal number of neighbors (k) to be used to maximize clustering of the relative (%) residential built up exposed to : coastal flood, flood, subsidence clustering (left side from upper to bottom plots) earthquake, landslides, forest fire_ WUI clustering (right side from upper to bottom plots)

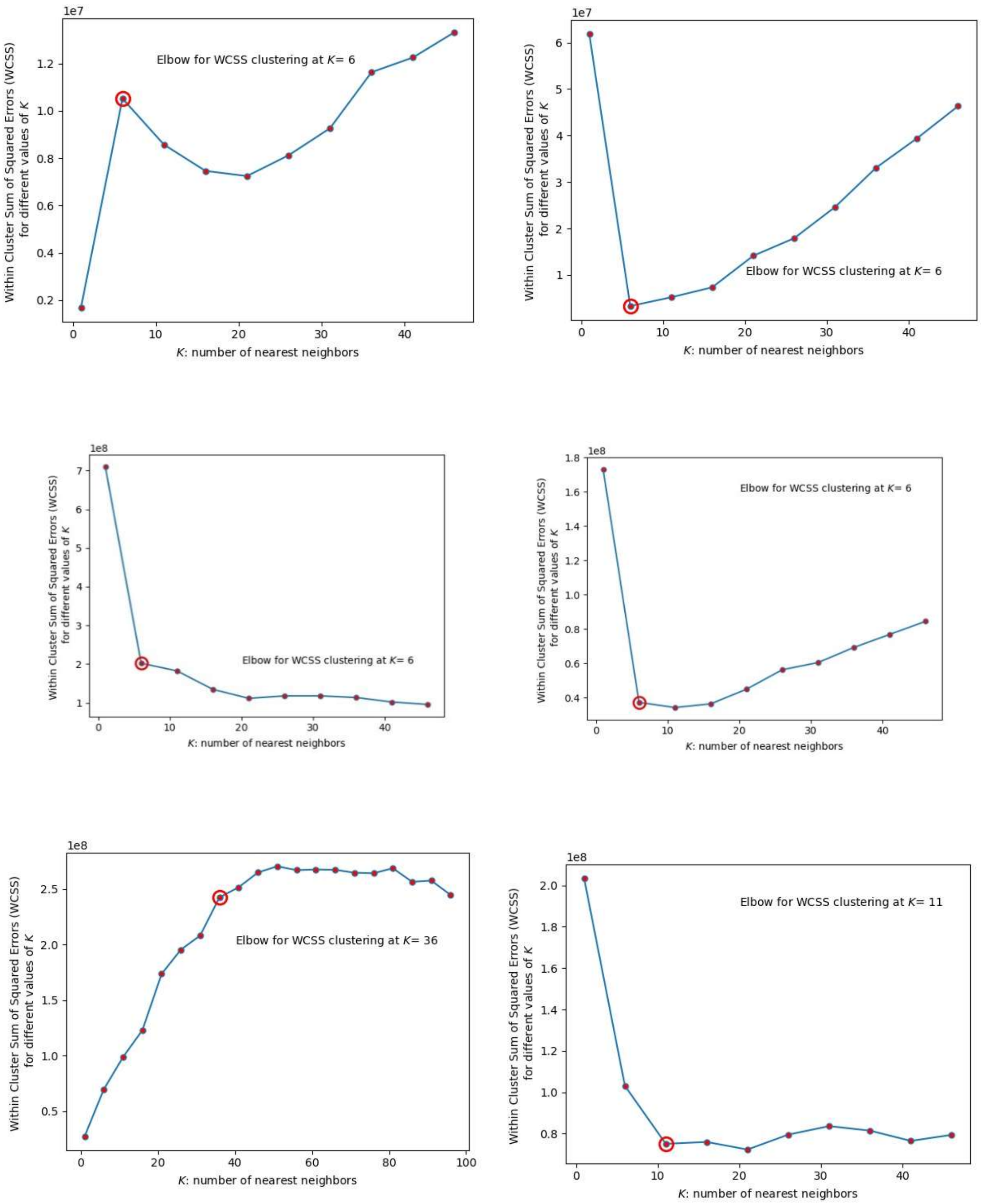

Figure S17. Elbow method applied on **WCSS coefficient**. The plots indicate the optimal number of neighbors (k) to be used to maximize clustering of the absolute residential built up exposed to : coastal flood, flood, subsidence clustering (left side from upper to bottom plots) earthquake, landslides, forest fire_ WUI clustering (right side from upper to bottom plots)

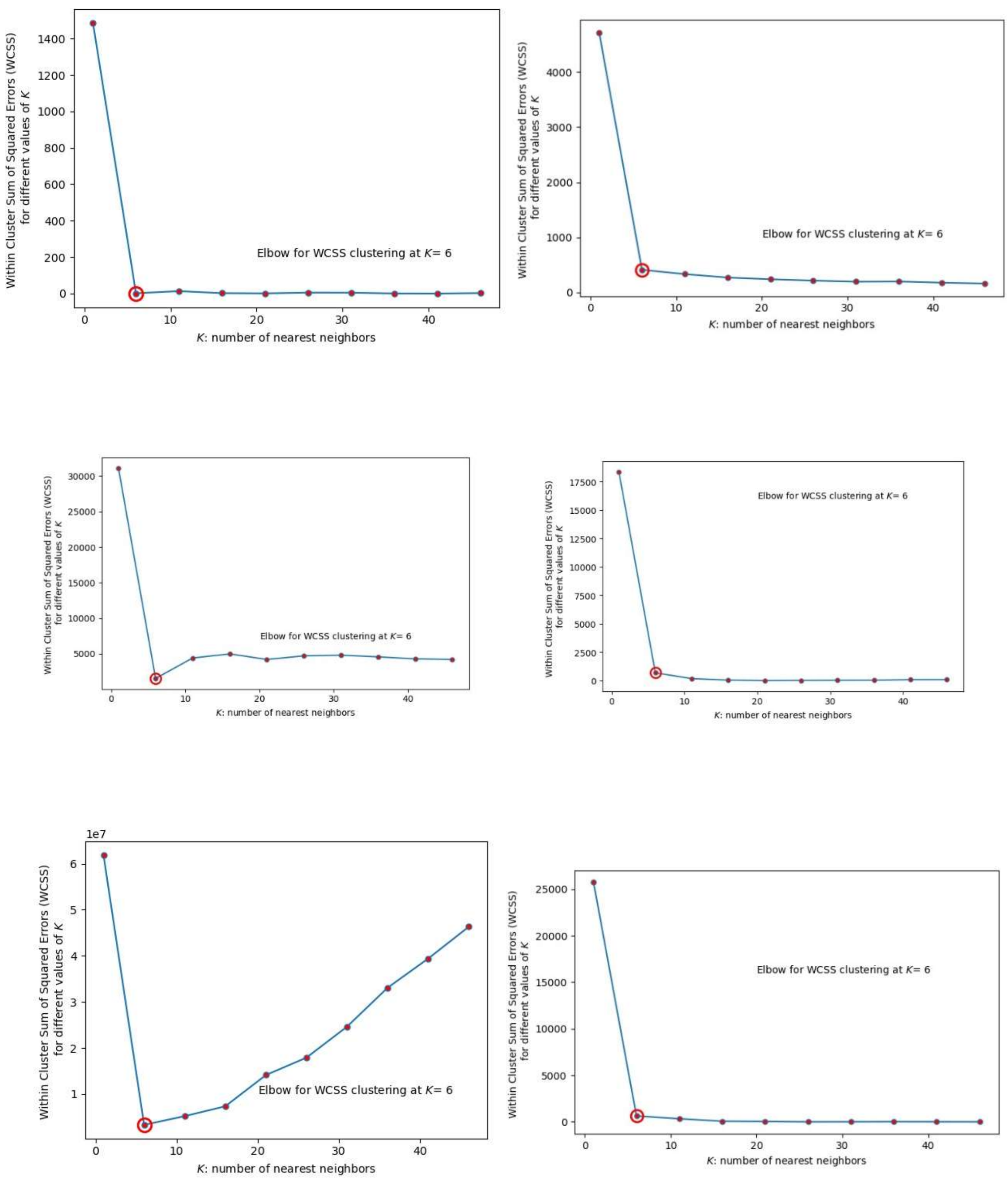

Figure S18. Elbow method applied on **MSE coefficient**. The plots indicate the optimal number of neighbors (k) to be used to maximize clustering of the relative (%) population exposed to : coastal flood, flood, subsidence clustering (left side from upper to bottom plots) earthquake, landslides, forest fire_ WUI clustering (right side from upper to bottom plots)

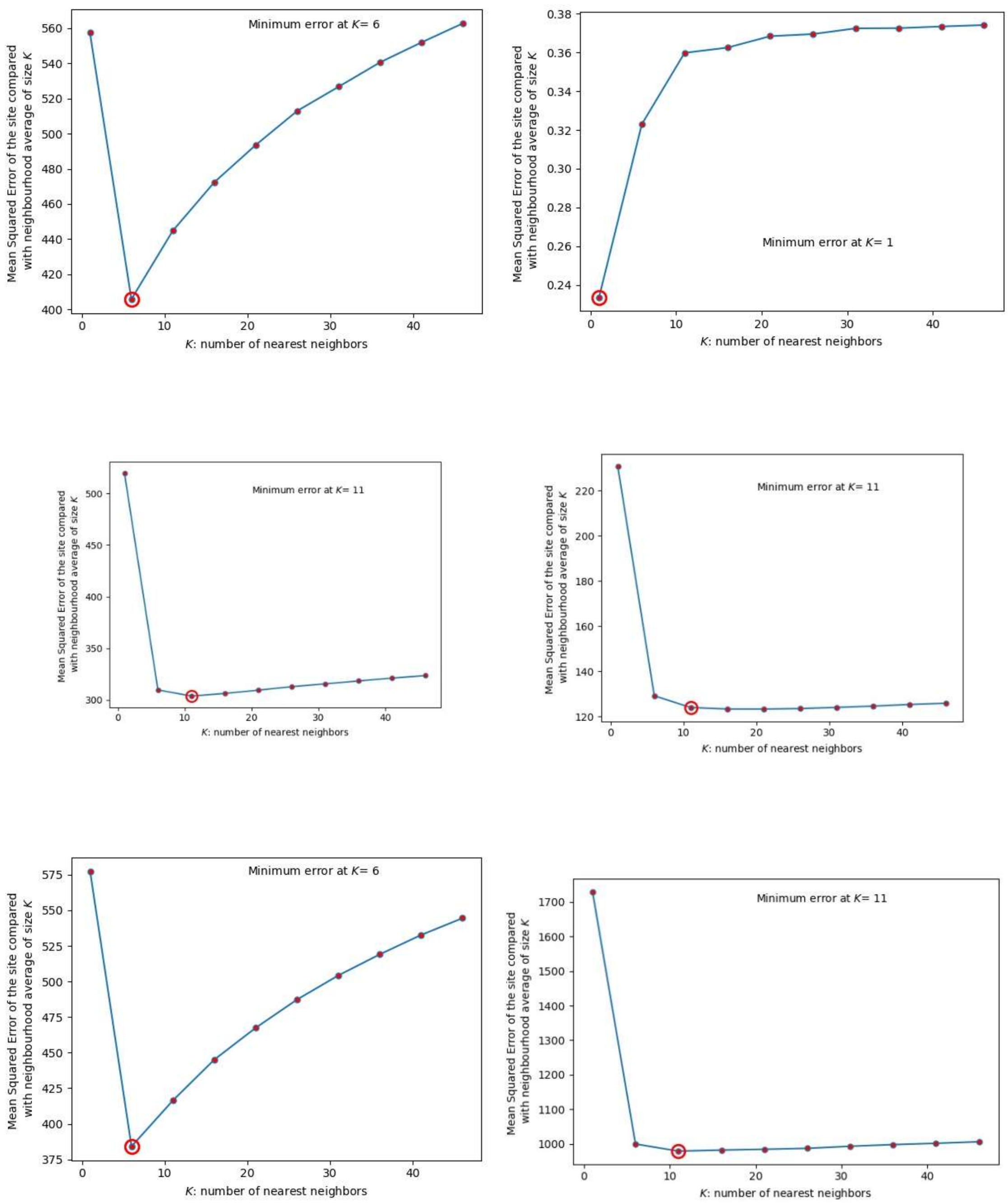

Figure S19. Elbow method applied on **MSE coefficient**. The plots indicate the optimal number of neighbors (k) to be used to maximize clustering of the absolute population exposed to : coastal flood, flood, subsidence clustering (left side from upper to bottom plots) earthquake, landslides, forest fire_ WUI clustering (right side from upper to bottom plots)

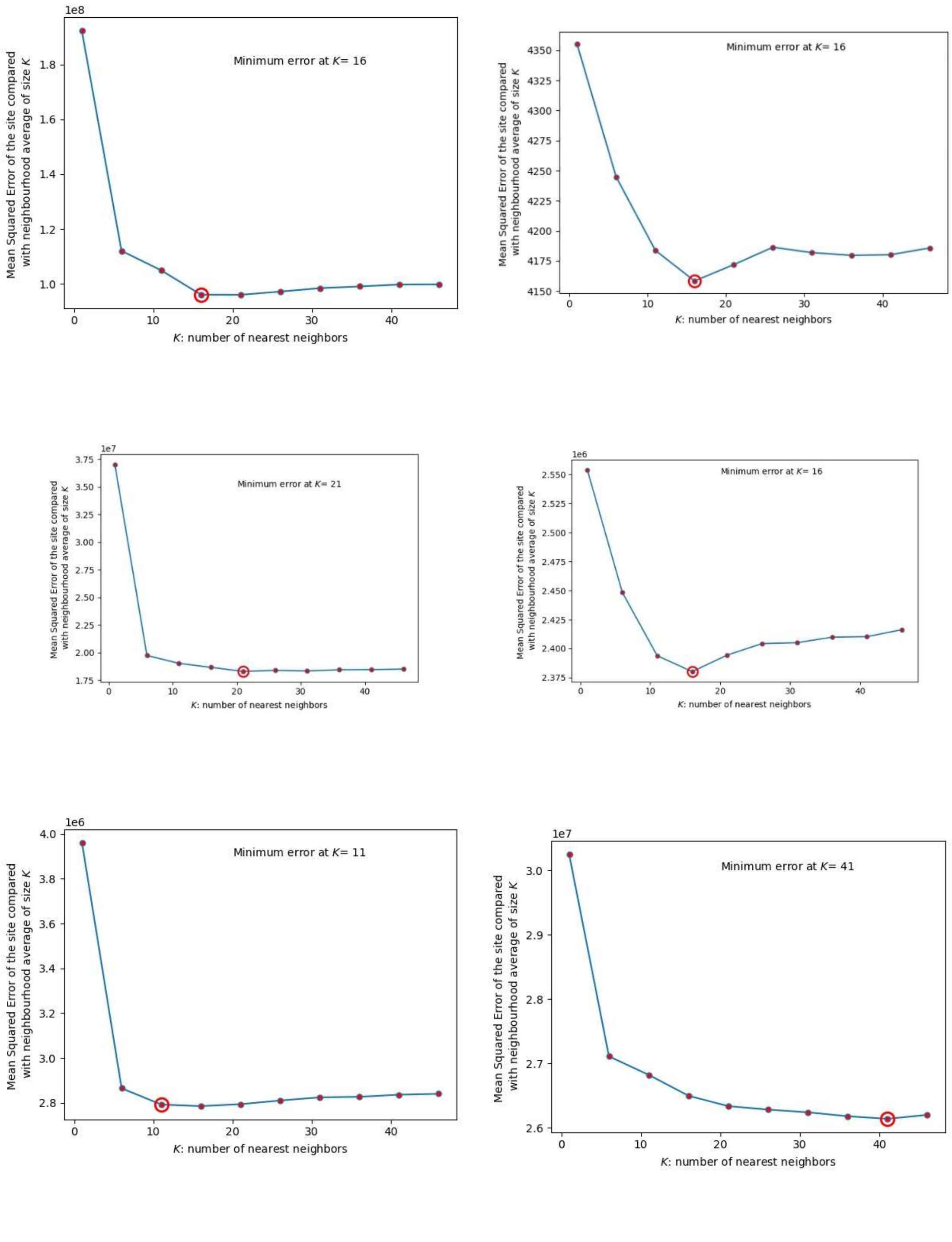

Figure S20. Elbow method applied on MSE coefficient. The plots indicate the optimal number of neighbors (k) to be used to maximize clustering of the relative (%) residential built up exposed to : coastal flood, flood, subsidence clustering (left side from upper to bottom plots) earthquake, landslides, forest fire_ WUI clustering (right side from upper to bottom plots)

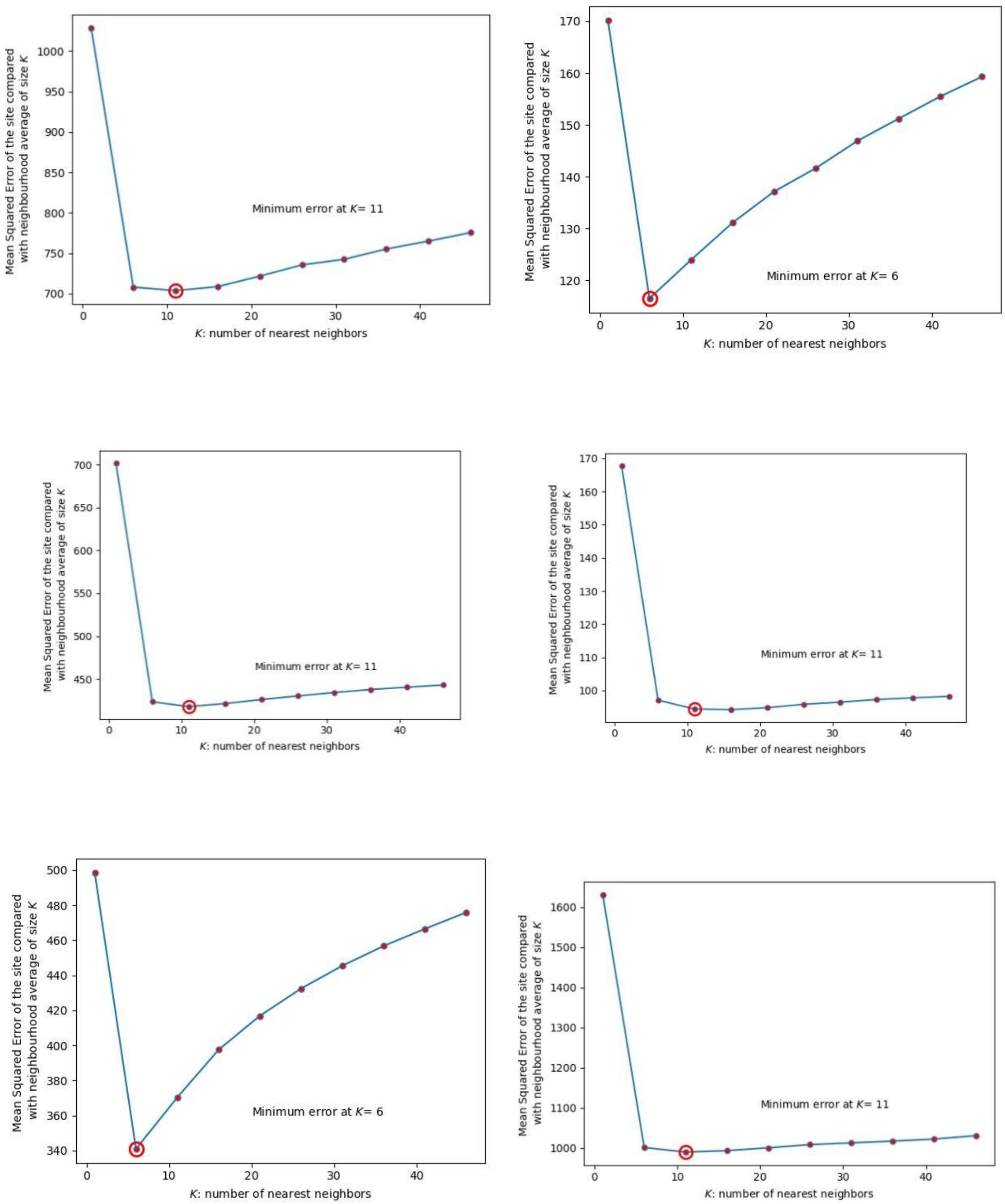

Figure S21. Elbow method applied on MSE coefficient. The plots indicate the optimal number of neighbors (k) to be used to maximize clustering of the absolute residential built up exposed to : coastal flood, flood, subsidence clustering (left side from upper to bottom plots) earthquake, landslides, forest fire_ WUI clustering (right side from upper to bottom plots)

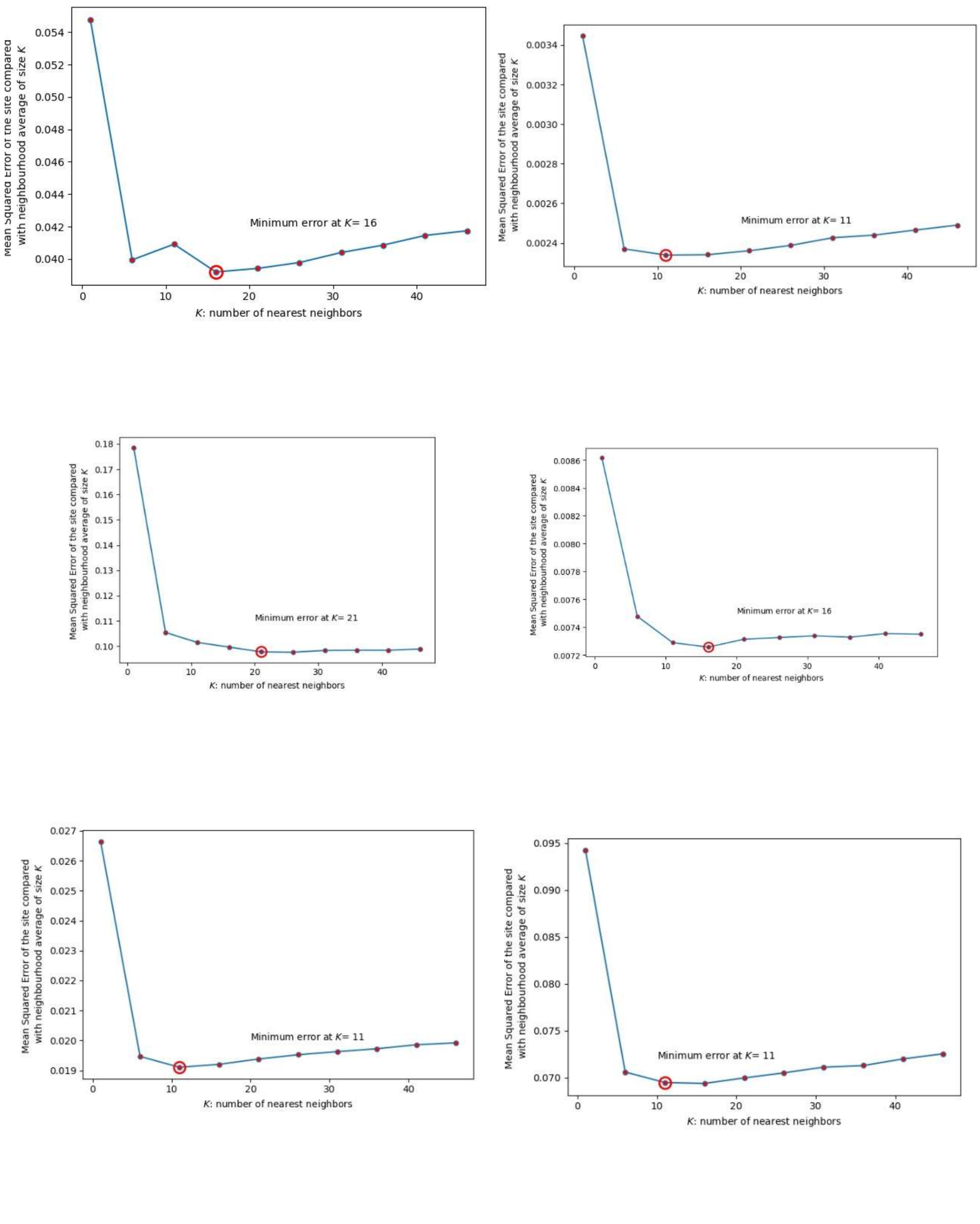

Figure S22. The distribution of the effect size (z-score) (upper plot) and the significance (bottom plot) of the methodologies used to compute the optima k for the single hazards considered (example of the relative (%) residential build up exposure)

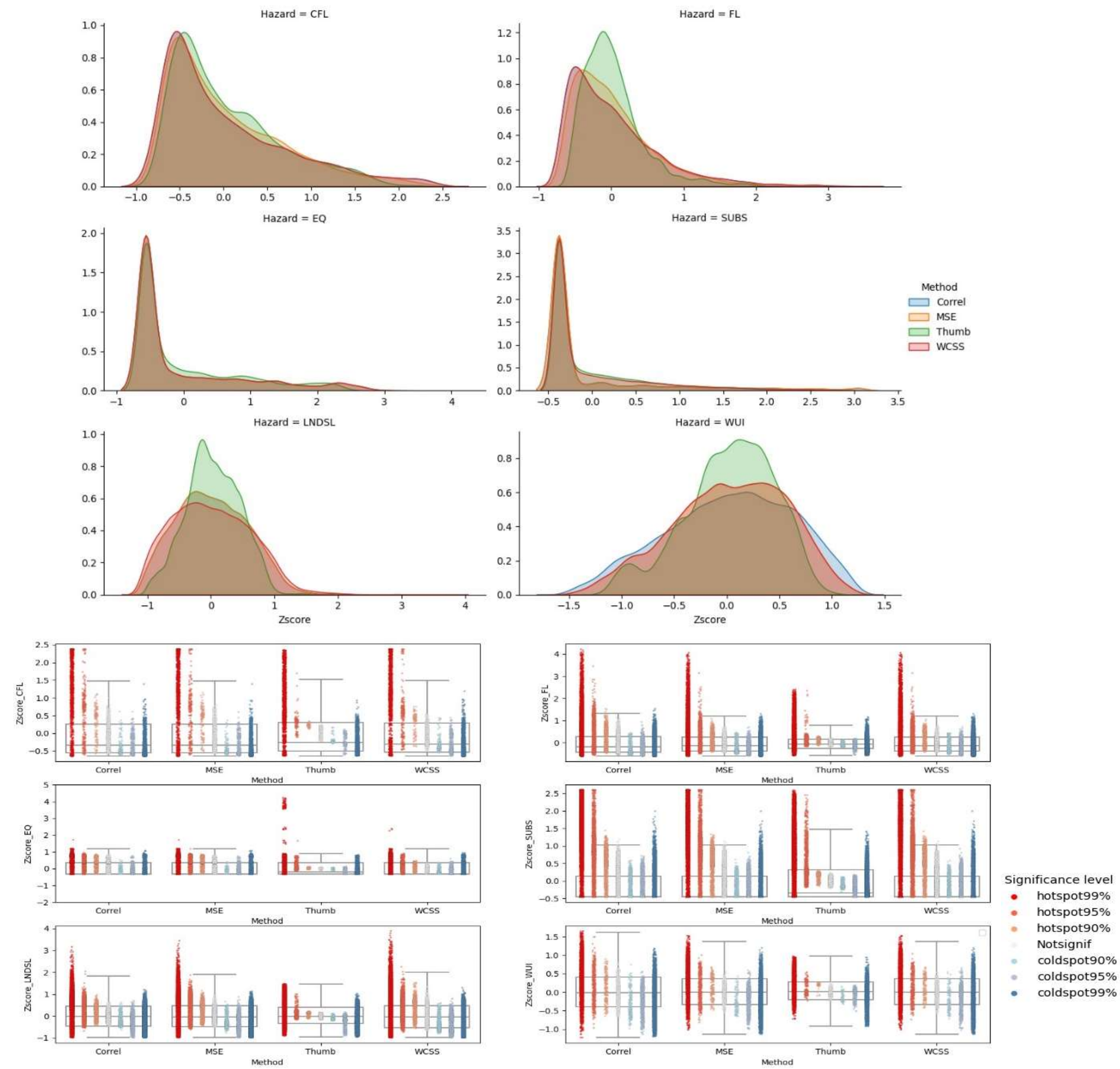

2.2 . Difference between the methodological aspects of the study and its implementation on the RDH platform

In contrast to other studies, transferability is not limited due to the reliance on case-study-specific data or methodology. The methodological approach described in this study it is already implemented on the DRMKC Risk Data Hub platform (https://drmkc.jrc.ec.europa.eu/risk-data-hub/#/). The methodology utilizes the existing analysis hosted and shared through the platform and demonstrates its accessibility and replicability. However, differences between the methodological approach presented and its implementation on the RDH platform exists. They are presented in the table S5 and they mainly include:

(i..) The input data. On the RDH the exposure as input is a matrix of exposure and probability on a temporal dimension (1, 5, 10, 15, 25 years) on which the cluster analysis are performed while in this study we only focused on a scenario (e.g. either medium case scenario: RP= 200yrs or an spatial probability/susceptibility: high, medium)

(ii..) The *(k)* parameter. The optimal neighbourhood size *(k)* used to cluster the single hazard exposure on the RDH platform is fixed to 8 neighbours whilst in the present study we use a dynamic *(k)* parameter function of the assets-hazard relation type (Supplementary , Section 2, table 3 and 4).

(iii.) The clustering. On the RDH platform, the statistical description of the cluster is based on the *Z*-score only while the study is underlying the statistical significance of the *Z*-score by considering the *p*-value. The implementation of the significance of the clusters is foreseen for the future development of the RDH platform.

(*iv*.) Meta analysis or the multi-hazard clustering (hot/cold-spots). Both the RDH platform and the present study use the Stouffer's method (Stouffer, 1949) based on unweighted *Z*-transform test.

(v.) Identification of regions at risk to multi-hazards. On the RDH platform is done only on the bases of the normalisation of the *Z*-score while in this study we consider for a statistical overview the regions with more than 1 hazard exposure (Hz > 1) and confidence level set at 90% (p-value < 0.10 and positive Z-score > 0).

Table S5. Difference between the methodological aspects of the study and its implementation on the RDH platform

Analysis		Risk Data Hub implemented methodology	Methodology presented in this article
		Single hazard exposure (E to Hz)	
1. Input data: Exposure		*f* (*t*, E to H) - Single hazard Expected Annual Exposure (matrix of exposure and probability on a temporal dimension)	(E to H) - Exposure to single hazard as scenario (as presented in table1)
2. Single hazard hot-spots (clustering)	Building a spatial weights matrix	**Kernel function**	
		With fixed neighbour size across all exposure type (k=8)	With dynamic neighbour size (*k*) computed for different types of

		exposures (Supplementary, Section 2, table 3 and 4)
Clustering	**Normalization using *Getis and Ord's Gi** as:**	
	- standard deviations (*Z*-score)	- standard deviations (*Z*-score); - probability (*p*-value)
3. Multi-hazard hot-spots (meta-analysis)	**Stouffer's method (Stouffer, 1949) based on Z-transform test**	
4. Identification of regions at risk to multi-hazards	Normalization of *Z*-scores (0-10)	Regions with more than 1 hazard exposure (Hz > 1) and confidence level set at 90% (*p*-value < 0.10 and positive *Z*-scores , Zs > 0)

Figure S23. Hot-spot analysis of multi-hazard population exposure at the level of urbanized areas (Functional Urban Area) in Europe .For the analysis in 3.1 (iii) only the high significant hot-spots are used (>90% confidence)

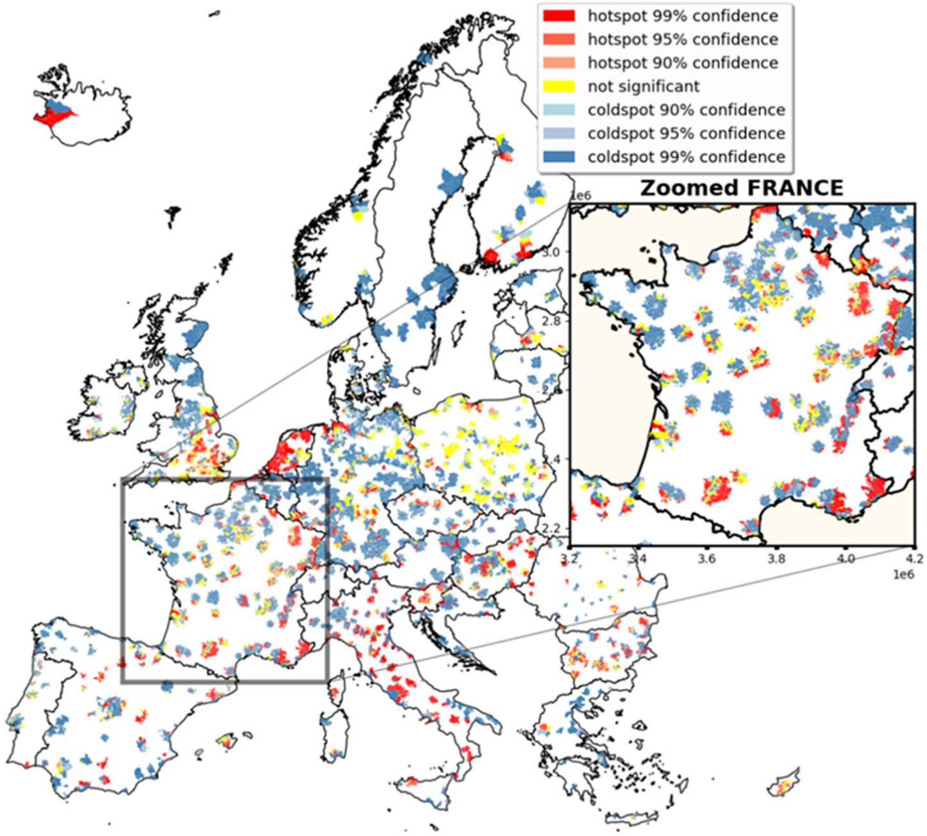

Table S6. Number of urban areas per income level and countries (only the high significant hot-spots are used : >90% confidence))

Countries	High income	High midle income	Low income	Low midle income	Total urban areas
AT	4	4		2	6
BE	2	3		3	6
BG			16		16
CH	8				8
CY				2	2
CZ			11		11
DE	20	26	1	20	49
DK	1	1			2
EL			1	1	2
ES	1	15	7	18	39
FI	5	2			7
FR	9	46		41	69
HR			4		4
HU			13		13
IE	2	2			3
IS	1				1

IT	9	30	8	25	63
LU	1				1
LV			3	1	3
NL	28	21		4	43
PL			15	1	15
PT			9	1	10
RO			17	1	17
SI			1	1	2
SK	1		5		6
UK	23	20		15	47
Grand Total	**115**	**169**	**110**	**136**	**442**

Figure S24. Population (%) at risk from multi-hazard risk occurrence within the urban areas comparing the categories: cities (or city cores/centers - C) and larger urbanized zones (commuting zone/Functional Urban - F).

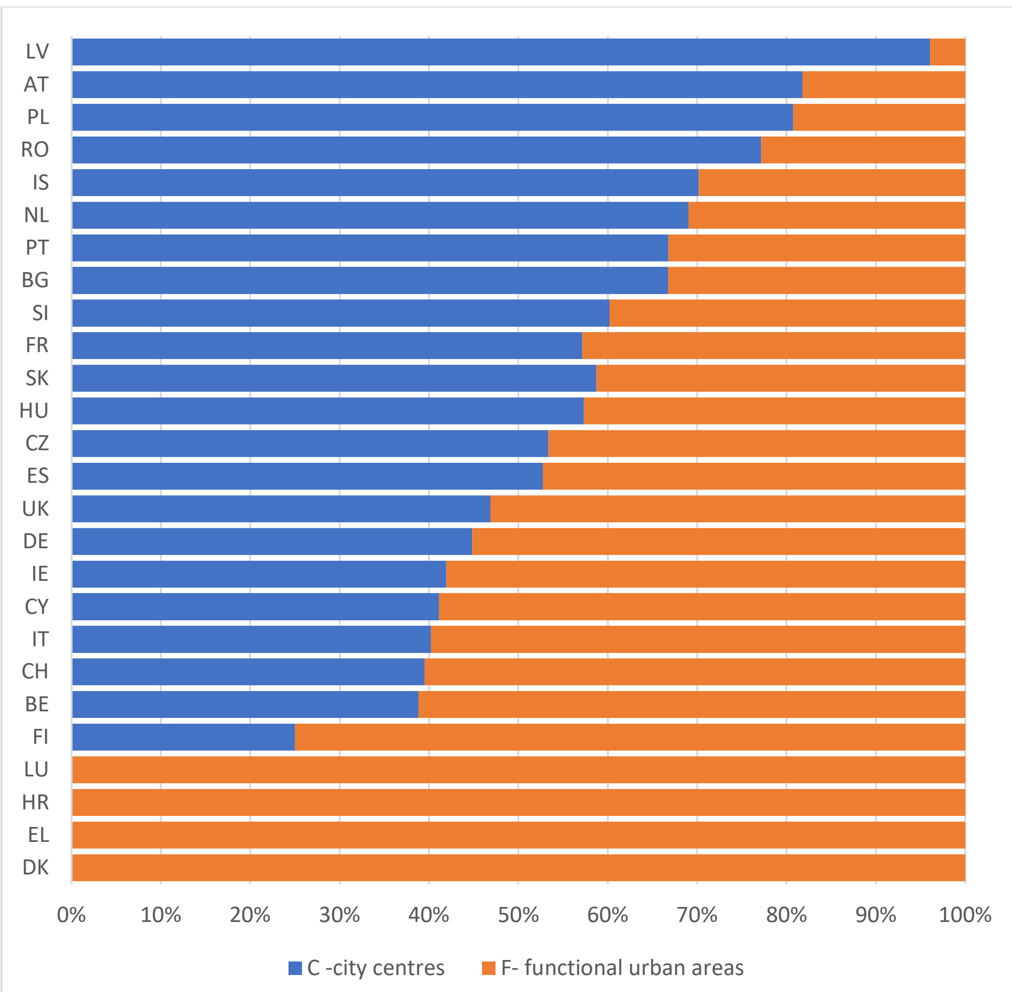

References

Alessandro Dosio, Lorenzo Mentaschi, Erich M Fischer, Klaus Wyser, 2018 Environ. Res. Lett. 13 054006, doi: 10.1088/1748-9326/aab827

Alfieri, L., Salamon, P., Bianchi, A., Neal, J., Bates, P., and Feyen, L.: Advances in pan-European flood hazard mapping, Hydrol. Process., 28, 4067–4077, doi:10.1002/hyp.9947, 2014

Alfieri, L., Feyen, L., Dottori, F., and Bianchi, A.: Ensemble flood risk assessment in Europe under high end climate scenarios, Global Environ. Change, 35, 199–212, doi:10.1016/j.gloenvcha.2015.09.004, 2015.

Alfieri, L., Feyen, L., and Baldassarre, G. D.: Increasing flood risk under climate change: a pan-European assessment of the benefits of four adaptation strategies, Climatic Change, 136, 507–521, doi:10.1007/s10584-016-1641-1, 2016.

UN-ISDR (2005), Hyogo framework for action 2005–1015: Building the resilience of nations and communities to disasters, in Final report of the World Conference on Disaster Reduction (A/CONF.206/6), Kobe, Hyogo, Japan.

Barnard, P. L., Short, A. D., Harley, M. D., Splinter, K. D., Vitousek, S., Turner, I. L., Allan, J., Banno, M., Bryan, K.R., Doria, A., Hansen, J. E., Kato, S., Kuriyama, Y., Randall-Goodwin, E., Ruggiero, P., Walker, I.J., and Heathfield, D.K. :Coastal vulnerability across the Pacific dominated by El Nino/Southern Oscillation, Nat. Geosci., 8, 801–807, 2015.

Bates, P. D., Horritt, M. S., and Fewtrell, T. J.: A simple inertial formulation of the shallow water equations for efficient two-dimensional flood inundation modelling, J. Hydrol., 387, 33–45, 2010.

Bertin, X., Bruneau, N., Breilh, J.-F., Fortunato, A. B., and Karpytchev, M.: Importance of wave age and resonance in storm surges: The case Xynthia, Bay of Biscay, Ocean Modell.,42,16– 30, 2012.

Birkmann J, Cardona OM, Carreño ML, Barbat AH, Pelling M, Schneiderbauer S, Kienberger S, Keiler M, Alexander D, Zeil P, Welle T (2013) Framing vulnerability, risk and societal responses: the MOVE framework. Nat Hazards 67(2):193–211.

Borenstein, M., Hedges, L. V., Higgins, J. P. T. and Rothstein, H. R. (2009) Front Matter, in Introduction to Meta-Analysis, John Wiley & Sons, Ltd, Chichester, UK. doi: 10.1002/9780470743386.

Brown, J., Wolf, J., and Souza, A.: Past to future extreme events in Liverpool Bay: model projections from 1960–2100, Climate Change, 111, 365–391, 2012.

Brown, S., Nicholls, R.J., Lowe, J.A., and Hinkel, J.: Spatial variations of sea-level rise and impacts: An application of DIVA, Climate Change, 134, 403–416, 2013.

Cabinet Office (2011) Keeping the country running: natural hazards and infrastructure. A guide to improving the resilience of critical infrastructure and essential services. Cabinet Office, London. https://www.gov.uk/government/uploads/system/uploads/attachment_data/file/61342/natural-hazards-infrastructure.pdf. Accessed 22 Mar 2015

Cardona, O.D., M.K. van Aalst, J. Birkmann, M. Fordham, G. McGregor, R. Perez, R.S. Pulwarty, E.L.F. Schipper, and B.T. Sinh, 2012: Determinants of risk: exposure and vulnerability. In: Managing the Risks of Extreme Events and Disasters to AdvanceClimate Change Adaptation [Field, C.B., V. Barros, T.F. Stocker, D. Qin, D.J. Dokken, K.L. Ebi, M.D. Mastrandrea, K.J. Mach,G.-K. Plattner, S.K. Allen, M. Tignor, and P.M. Midgley (eds.)]. A Special Report of Working Groups I and II of the Intergovernmental Panel on Climate Change (IPCC). Cambridge University Press, Cambridge, UK, and New York, NY, USA, pp. 65-108.

Chen, Z. 2011. Is the weighted z-test the best method for combining probabilities from independent tests? Journal of Evolutionary Biology 24: 926–930.

Jaedicke, C., Van Den Eeckhaut, M., Nadim, F. et al. 2014. Identification of landslide hazard and risk ‘hotspots’ in Europe, Bull Eng Geol Environ (2014) 73: 325. https://doi.org/10.1007/s10064-013-0541-0

Corbane, C., Hancilar, U., Ehrlich, D., De Grove, T., 2017, Pan-European seismic risk assessment: a proof of concept using the Earthquake Loss Estimation Routine (ELER), Bull Earthquake Eng., 15: 1057. https://doi.org/10.1007/s10518-016-9993-5.

Corti, T., Wues,t M., Bresch, D., Seneviratne, S.I., (2011) Drought-induced building damages from simulations at regional scale. Nat Hazards Earth Syst Sci 11:3335–3342

De Pippo, T., Donadio, C., Pennetta, M., Petrosino, C., Terlizzi, F., and Valente, A.: Coastal hazard assessment and mapping in Northern Campania, Italy, Geomorphology, 97, 451- 466, doi:10.1016/j.geomorph.2007.08.015, 2008.

di Mauro, M., de Bruijn, K.M., Meloni, M. (2012) Quantitative methods for estimating flood fatalities: towards the introduction of loss-of-life estimation in the assessment of flood risk. Natural Hazards, Vol. 63, 1083 - 1113.

Dilley, M., Chen, R. S., Deichmann, U., Lerner-Lam, A. L., and Arnold, M.: Natural Disaster Hotspots, a global risk analysis, the World Bank, p. 112, p. 132, 2005.

Dunford R, Harrison PA, Jager J, Rounsevell MDA, Tinch R (2014) Exploring climate change vulnerability across sectors and scenarios using indicators of impacts and coping capacity. Clim Chang. doi:10.1007/s10584-014-1162-8

Elmer, F., Hoymann, J., Düthmann, D., Vorogushyn, S., Kreibich, H., 2012. Drivers of flood risk change in residential areas Natural Hazards and Earth System Science, 12 (2012), pp. 1641-1657, 10.5194/nhess-12-1641-2012

Falter, D., Dung, N. V., Vorogushyn, S., Schröter, K., Hundecha, Y., Kreibich, H., Apel, H., Theisselmann, F., and Merz, B.: Continuous, large-scale simulation model for flood risk assessments: proof-of-concept, J. Flood Risk Manage., 9, 3–21, doi:10.1111/jfr3.12105, 2016.

Faenza L, Michelini A (2010) Regression analysis of MCS intensity and ground motion parameters in Italy and its application in ShakeMap. Geophys J Int 180:1138–1152. doi: 10.1111/j.1365-246X.2009.04467.x

Feyen, L., Dankers, R., Bódis, K., Salamon, P., and Barredo, J. I.: Fluvial flood risk in Europe in present and future climates, Climatic Change, 112, 47–62, 2012

Fisher, R. 1932. Statistical methods for research workers. Oliver and Boyd, Edinburgh.

Gallina, V., Torresan, S., Critto, A., Sperotto, A., Glade, T., Marcomini, A., 2016. A review of multi-risk methodologies for natural hazards: consequences and challenges for a climate change impact assessment. J. Environ. Manage. 168, 123-132, https://doi.org/10.1016/j.jenvman.2015.11.011.

Garcia, R. A. C., Oliveira, S. C., and Zêzere, J. L.: Assessing population exposure for landslide risk analysis using dasymetric cartography, Nat. Hazards Earth Syst. Sci., 16, 2769-2782, https://doi.org/10.5194/nhess-16-2769-2016, 2016.

Gaslikova, L., Grabemann, I., and Groll, N.: Changes in North Sea storm surge conditions for four transient future climate realizations, Nat. Hazards, 66, 1501–1518, 2013

Gill, J. C. and Malamud, B. D.: Reviewing and visualizing the interactions of natural hazards, Rev. Geophys., 52, 680–722, 2014.

Getis, A. and Ord, J. K. (1992), The Analysis of Spatial Association by Use of Distance Statistics. Geographical Analysis, 24: 189–206. doi:10.1111/j.1538-4632.1992.tb00261.x

Glade T, Kappes MS, Frigerio S, Malet JP (2012) Multi-hazard exposure analyses with multirisk—a platform for user-friendly analysis. 12th Congress INTERPRAEVENT, Grenoble, France, pp 487–495
Granger, K., Jones, T., Leiba, M., & Scott, G. (1999). Community Risk in Cairns: A Multi-Hazard Risk Assessment. Canberra: Commonwealth of Australia Publishing.

Greiving, S., Fleischhauer, M., and Lückenkötter, J.: A methodology for an integrated risk assessment of spatially relevant hazards, J. Environ. Plann. Man., 49, 1–19, 2006.

Grünthal, G., Thieken, A. H., Schwarz, J., Radtke, K. S., Smolka,A., and Merz, B.: Comparative risk assessment for the city of Cologne-storms, floods, earthquake, Nat. Hazards, 38, 21–44, 2006.

Wilde, M., Günther, A., Reichenbach, P., Malet, J.-P., Hervás, J., 2018. Pan-European landslide susceptibility mapping: ELSUS Version 2. Journal of Maps, 14(2): 97-104 and supplemental map.

Guzzetti F., Carrara A., Cardinali M., Reichenbach P.1999, Landslide hazard evaluation: a review of current techniques and their application in a multi-scale study, Central Italy Geomorphology, 31 (1999), pp. 181-216

Guzzetti, F., (2000) Landslide fatalities and the evaluation of landslide risk in Italy. Eng Geol 58:89–107

Hewitt, K. and Burton, I. (1971) The Hazardousness of a Place: A Regional Ecology of Damage Events, University of Toronto Press.

Han, J., Wu, S., and Wang, H.: Preliminary study on geological hazard chains, Earth Science Frontiers, 14, 11–20, doi:10.1016/S1872-5791(08)60001-9, 2007.

Hinkel, J., Nicholls, R., Vafeidis, A., Tol, R. J., and Avagianou, T.: Assessing risk of and adaptation to sea-level rise in the European Union: an application of DIVA, Mitig. Adapt. Strateg. Glob. Change, 15, 703–719, 2010.

Hinkel, J., Lincke, D., Vafeidis, A. T., Perrette, M., Nicholls, R. J., Tol, R. S. J., Marzeion, B., Fettweis, X., Ionescu, C., and Levermann, A.: Coastal flood damage and adaptation costs under 21st century sea-level rise, P. Natl. Acad. Sci. USA, 111, 3292–3297, 2014.

Jakob, M., Hungr, O. 2015 Debris-flow Hazards and related phenomena, Springer-Praxis book in Geophysical Sciences, doi 10.1007/b138657 , 739, Springer-Verlag Berlin Heidelberg, New York.

IPCC (2012) Managing the risks of extreme events and disasters to advance climate change adaptation. A special report of working groups I and II of the intergovernmental panel on climate change. Cambridge University Press, Cambridge.

Jongman, B., Hochrainer-Stigler, S., Feyen, L., Aerts, J. C. J. H., Mechler, R., Botzen, W. J. W., Bouwer, L. M., Pflug, G., Rojas, R., and Ward, P. J.: Increasing stress on disaster-risk finance due to large floods, Nat. Clim. Change, 4, 264–268, doi:10.1038/nclimate2124, 2014

Jonkman, S.N., Maaskant, B., Kolen, B., Needham, J.T., Loss of life estimation – Review, developments and challenges, E3S Web Conf. 7 06004 (2016), DOI: 10.1051/e3sconf/20160706004

JORF n°164 du 17. LOI no 92-665 du 16 juillet 1992 portant adaptation au marché unique européen de la législation applicable en matière d'assurance et de crédit (https://www.legifrance.gouv.fr/)

Kappes, M. S., Keiler, M., and Glade, T.: From single- to multi-hazard risk analyses: a concept addressing emerging challenges, in: Mountain Risks: Bringing Science to Society, edited by: Malet, J. P., Glade, T., and Casagli, N., CERG Editions, Strasbourg, France, 351–356, 2010.

Kappes M.S., Gruber, K., Frigerio, S., Bell, R., Keiler, M., Glade, T. 2012. The multirisk platform: the technical concept and application of a regional-scale multihazard exposure analysis tool. Geomorphology 151–152:139–155. doi:10.1016/j.geomorph.2012.01.024

Kappes, M. S., Keiler, M., von Elverfeldt, K., and Glade, T.: Challenges of analyzing multi-hazard risk: a review, Nat. Hazards, 64,1925–1958, 2012

Kolen, B., Kok, M., Helsloot, I., Maaskant, B., (2012) EvacuAid: a probabilistic evacuation model to determine the expected loss of life for different mass evacuation strategies. Risk Analysis doi: 10.1111/j.1539-6924.2012.01932.x.

Lesser, G. R., Roelvink, J. A., van Kester, J. A. T. M., and Stelling, G. S.: Development and validation of a three-dimensional morphological model, Coast. Eng., 51, 883–915, 2004.

Lloyd, S. J., Kovats, R. S., Chalabi, Z., Brown, S., and Nicholls, R.J.: Modelling the influences of climate change-associated sea level rise and socioeconomic development on future storm surge mortality, Climate Change, 134, 441–455, 2015.

Lowe, J. A., Howard, T. P., Pardaens, A., Tinker, J., Holt, J., Wakelin, S., Milne, G., Leake, J., Wolf, J., Horsburgh, K., Reeder, T., Jenkins,G.,Ridley,J.,Dye,S.,andBradley,S.:UKClimateProjections science report: Marine and coastal projections, Met Office Hadley Centre, Exeter, UK, 2009.

Losada, I. J., Reguero, B. G., Méndez, F. J., Castanedo, S., Abascal, A. J., and Mínguez, R.: Long-term changes in sea-level components in Latin America and the Caribbean, Global Planet. Change, 104, 34–50, 2013.

Lipták, T. 1958. On the combination of independent tests. Magyar Tud. Akad. Mat. Kutato Int. Közl3: 171–196

Marzocchi, W., Mastellone, M., Di Ruocco, A., Novelli, P., Romeo,E., and Gasparini, P.: Principles of Multi-Risk Assessment: Interactions Amongst Natural and Man-Induced Risks, European Commission, Directorate-General for Research, Environment Directorate, Luxembourg, 72 pp., 2009

Marzocchi, W., Garcia-Aristizabal, A., Gasparini, P., Mastellone,M., and Di Ruocco, A.: Basic principles of multi-risk assessment: a case study in Italy, Nat. Hazards, 62, 551–573, 2012.

Mahendra, R. S., Mohanty, P. C., Bisoyi, H., Kumar, T. S., and Nayak, S.: Assessment and management of coastal multi-hazard vulnerability along the Cuddalore–Villupuram, east coast of India using geospatial techniques, Ocean Coast. Manage., 54, 302–311, doi:10.1016/j.ocecoaman.2010.12.008, 2011.

M. Smid, S. Russo, A.C. Costa, C. Granell, E. Pebesma, Ranking European capitals by exposure to heat waves and cold waves, Urban Climate, Volume 27, 2019, Pages 388-402, ISSN 2212-0955, https://doi.org/10.1016/j.uclim.2018.12.010.

McCall, R. T., Van Thiel de Vries, J. S. M., Plant, N. G., Van Dongeren, A. R., Roelvink, J. A., Thompson, D. M., and Reniers, A. J. H. M.: Two-dimensional time dependent hurricane overwash and erosion modeling at Santa Rosa Island, Coast. Eng., 57, 668–683, 2010.

Merz, B., Kreibich, H., Schwarze, R., and Thieken, A.: Review article "Assessment of economic flood damage", Nat. Hazards Earth Syst. Sci., 10, 1697-1724, https://doi.org/10.5194/nhess-10-1697-2010, 2010.

De Moel, H., Aerts, J.C.J.H. (2011) Effect of uncertainty in land use, damage models and inundation depth on flood damage estimates. Nat Hazards 58(1):407–425

Murphy, J., R. 1978. Analysis of a worldwide strong motion data sample to develop an improved correlation between peak acceleration, seismic intensity and other physical parameters/. Nuclear Regulatory Commission, Office of Standards Development, Washington

Trifunac MD, Brady AG (1976) Correlations of peak acceleration, velocity and displacement with earthquake magnitude, distance and site conditions. Earthq Eng Struct Dyn 4:455–471. doi: 10.1002/eqe.4290040504

Musson, R., M.,W., 2000. Intensity-based seismic risk assessment, Soil Dynamics and Earthquake Engineering, Volume 20, Issues 5–8, 2000, Pages 353-360, ISSN 0267-7261, https://doi.org/10.1016/S0267-7261(00)00083-X. (http://www.sciencedirect.com/science/article/pii/S026772610000083X)

Papathoma-Köhle M, Neuhäuser B, Ratzinger K, Wenzel H, Dominey-Howes D (2007) Elements at risk as a framework for assessing the vulnerability of communities to landslides. Nat Hazards Earth Syst Sci 7:765–779

Papathoma-Köhle, M., Kappes, M., Keiler, M., Glade, T. (2011) Physical vulnerability assessment for alpine hazards: state of the art and future needs. Nat Hazards 58:645–680. doi: 10.1007/s11069-010-9632-4,

Pellicani R, Van Westen C, Spilotro G (2013) Assessing landslide exposure in areas with limited landslide information. Landslides 11:463–480. doi: 10.1007/s10346-013-0386-4

Promper C, Gassner C, Glade T (2015) Spatiotemporal patterns of landslide exposure—a step within future landslide risk analysis on a regional scale applied in Waidhofen/Ybbs Austria. Int J Disaster Risk Reduct 12:25–33. doi:10.1016/j.ijdrr.2014.11.003

Promper, C. & Glade, T., 2016, Multilayer-exposure maps as a basis for a regional vulnerability assessment for landslides: applied in Waidhofen/Ybbs, AustriaNat Hazards, 82(Suppl 1): 111. https://doi.org/10.1007/s11069-016-2311-3

Pritchard, O.G., Hallett, S.H. and Farewell, T.S. (2013) Soil movementin the UK –Impacts on Critical Infrastructure. 74 pp. NSRI, Cranfield University, UK.

Preston, B. , D., Abbs, B., Beveridge, C., Brooke, Gorddard R, Hunt G, Justus M, Kinrade P, Macadam L, Measham T G,McInnes K, Morrison C, O'Grady J, Smith T F and Withycombe G 2007 Spatial approaches for assessing vulnerability and consequences in climate change assessments Modelling & Simulation Society of Australia & New Zealand 261.

Reason J., 1990, Human error. New York: Cambridge University Press; 1990.

Roelvink, D., Reniers, A., Dongeren, A. V., Vries, J. V. T. D., McCall, R., and Lescinski, J.: Modelling storm impacts on beaches, dunes and barrier islands, Coast. Eng., 56, 1133–1152, 2009.

Rojas, R., Feyen, L., Bianchi, A., Dosio, A., 2012. Assessment of future flood hazard in Europe using a large ensemble of bias-corrected regional climate simulations Journal of Geophysical Research, 117 (2012), p. D17109, 10.1029/2012JD017461.

Rojas, R., Feyen, L., and Watkiss, P.: Climate change and river floods in the European Union: Socio-economic consequences and the costs and benefits of adaptation, Global Environ. Change, 23, 1737–1751, doi:10.1016/j.gloenvcha.2013.08.006, 2013

San-Miguel-Ayanz, J., Schulte, E., Schmuck, G., Camia, A., 2013. The European Forest Fire Information System in the context of environmental policies of the European Union, In Forest Policy and Economics, Volume 29, Pages 19-25, ISSN 1389-9341, https://doi.org/10.1016/j.forpol.2011.08.012.

Seed, H.B., Woodward, R.J., Lundgren. R., (1962) Prediction of swelling potential for compacted clays. J Soil Mech Foundation Div (ASCE) 88(3):53–87

Schneider, S. H., Semenov, S., Patwardhan, A., Burton, I., Magadza, C. H.D., Oppenheimer, M., Pittock, A. B., Rahman, A., Smith, J.B., Suarez, A., and Yamin, F. (2007), Assessing Key Vulnerabilities and the Risk from Climate

Change. In: Climate Change 2007: Impacts, Adaptation and Vulnerability.Contribution of Working Group II to the Fourth Assessment Report of the Intergovernmental Panel on Climate Change (M .L. Parry, O.F. Canziani, J.P. Palutikof, P.J. van der Linden and C.E. Hanson, Eds.). Cambridge University Press, Cambridge, UK.

Schumann, G. J.-P., Neal, J. C., Voisin, N., Andreadis, K. M., Pappenberger, F., Phanthuwongpakdee, N., Hall, A. C., and Bates, P.D.: A first large-scale flood inundation forecasting model, Water Resour. Res., 49, 6248–6257, doi:10.1002/wrcr.20521, 201

Seenath, A., Wilson, M., and Miller, K.: Hydrodynamic versus GIS modelling for coastal flood vulnerability assessment: Which is better for guiding coastal management?, Ocean Coast. Manag., 120, 99–109, 2016.

Smyth, P., "Clustering using Monte Carlo Cross Validation" , In Proc.2nd Intl. Conf. Knowl. Discovery and Data Mining (KDD-96), Portland, 1996.

Salagnac, J. L., 2007: Lessons from the 2003 heat wave: a French per-spective, Build. Res. Informat., 35, 450–457, 2007

Steinberg M (1998) Geomembranes and the control of expansive soils in construction. McGraw-Hill, New York, p 222

Sudjianto, A. T., Suryolelono, K. B, Rifa'I, A., and Mochtar, I. B., (2011), The effect of variation index plasticity and activity in swelling vertical of expansive soil. International journal of Engeneering & Technology IJET-IJENS, Vol. 11, No. 6, pp. 142-148.

Tarvainen, T., Jarva, J., and Greiving, S.: Spatial pattern of hazards and hazard interactions in Europe, in: Natural and Technological Hazards and Risks Affecting the Spatial Development of European Regions, edited by: Schmidt-Thomé, P., Geological Survey Of Finland, Espoo, Finland, 42, 83–91, 2006

te Linde, A. H., Bubeck, P., Dekkers, J. E. C., de Moel, H.,and Aerts, J. C. J. H.: Future flood risk estimates along the river Rhine, Nat. Hazards Earth Syst. Sci., 11, 459–473, doi:10.5194/nhess-11-459-2011, 2011.

Teselentis, G., A, Danciu, L (2008) Empirical relationships between modified mercalli intensity and engineering ground-motion parameters in Greece. Bull Seismol Soc Am 98:1863–1875. doi: 10.1785/0120070172.

Thiebes, Benni & Bai, Shibiao & Xi, Yanan & Glade, Thomas & Bell, Rainer. (2017). Combining landslide susceptibility maps and rainfall thresholds using a matrix approach. Revista de Geomorfologie. 19. 58-74. 10.21094/rg.2017.003.

Van der Merve, D.H. (1964) The prediction of heave from the plasticity index and the percentage clay fraction of soils. Civil Eng S Afr 6:103–107

van Westen, C. J., Montoya, L., Boerboom, L., & Badilla Coto, E. (2002). Multi-hazard risk assessment using GIS in urban areas: a case study for the city of Turrialba, Costa Rica. 120-136.

van Westen C., Kappes M.S., Luna B.Q., Frigerio S., Glade T., Malet JP. (2014) Medium-Scale Multi-hazard Risk Assessment of Gravitational Processes. In: Van Asch T., Corominas J., Greiving S., Malet JP., Sterlacchini S. (eds) Mountain Risks: From Prediction to Management and Governance. Advances in Natural and Technological Hazards Research, vol 34. Springer, Dordrecht

Veerbeek W and Husson H 2013 Vulnerability to Climate Change: Appraisal of a vulnerability assessment method in a policy context. KfC report number 98/2013 (Unesco-IHE OR/MST/177)

Vousdoukas, M. I., Ferreira, O., Almeida, L. P., and Pacheco, A.: Toward reliable storm-hazard forecasts: XBeach calibration and its potential application in an operational early-warning system, Ocean Dynam., 62, 1001–1015, 2012.

Vousdoukas, M. I., Voukouvalas, E., Mentaschi, L., Dottori, F., Giardino, A., Bouziotas, D., Bianchi, A., Salamon, P., and Feyen, L.: Developments in large-scale coastal flood hazard mapping, Nat. Hazards Earth Syst. Sci., 16, 1841-1853, https://doi.org/10.5194/nhess-16-1841-2016, 2016

Wald DJ, Quitoriano V, Heaton TH, Kanamori H (1999) Relationships between peak ground acceleration, peak ground velocity, and modified mercalli intensity in California. Earthq.Spectra 15:557–564. doi: 10.1193/1.1586058

Ward, P.J., de Moel,H., Aerts, J.C.J.H., How are flood risk estimates affected by the choice of return-periods? Natural Hazards and Earth System Science, 11 (2011), pp. 3181-3195, 10.5194/nhess-11-3181-2011

Weisse, R., Bellafiore, D., Menéndez, M., Méndez, F., Nicholls, R. J., Umgiesser, G., and Willems, P.: Changing extreme sea levels along European coasts, Coast. Eng., 87, 4–14, 2014.

Wüest. M., Bresch, D., Corti, T., 2011, The hidden risks of climate change: an increase in property damage from soil subsidence in Europe, Swiss Re Media Production, Zurich, Order no: 1504390_11_en.

Wipulanusat, W., Nakrod, S., Prabnarong, P. (2009). Multi - hazard risk assessment using GIS and RS applications: a case study of Pak Phanang basin. Walailak Journal of Science and Technology 6, 109 - 125.

Whitlock, M.C. 2005. Combining probability from independent tests: the weighted Z-method is superior to Fisher's approach. Journal of Evolutionary Biology 18: 1368–1373.

Worden, C.B. and D.J. Wald (2016). ShakeMap Manual Online: technical manual, user's guide, and software guide, U. S. Geological Survey. usgs.github.io/shakemap. DOI: 10.5066/F7D21VPQ.

Woessner J, Giardini D, Crowley H, Cotton F, Grünthal G, Valensise G, Arvidsson R, Basili R, Demircioglu MB, Hiemer S, Meletti C, Musson RW, Rovida AN, Sesetyan K, Stucchi M (2015) The 2013 European seismic hazard model: key components and results. Bull Earthq Eng. doi: 10.1007/s10518-015-9795-1

Stouffer, S., DeVinney, L. & Suchman, E. 1949. The American soldier: Adjustment during army life, vol. 1. Princeton University Press Princeton, US.

Zaykin, D., Zhivotovsky, L., Westfall, P. & Weir, B. 2002. Truncated product method for combining P-values. Genetic Epidemiology 22: 170–185.

Zêzere, J.L., Garcia, RA.,C., Oliveira, S.C., Reis, E. (2008) Probabilistic landslide risk analysis considering direct costs in the area north of Lisbon (Portugal). Geomorphology 94:467–495. doi: 10.1016/j.geomorph.2006.10.040